CLASSIFICATION OF DAMAGED BUILDINGS IN AERIAL OBLIQUE IMAGES AND LASER SCANNING DATA

OGUT JOSEPH CYPRIAN

March, 2013

SUPERVISORS:

Dr. M. Gerke

Dr. K. Khoshelham

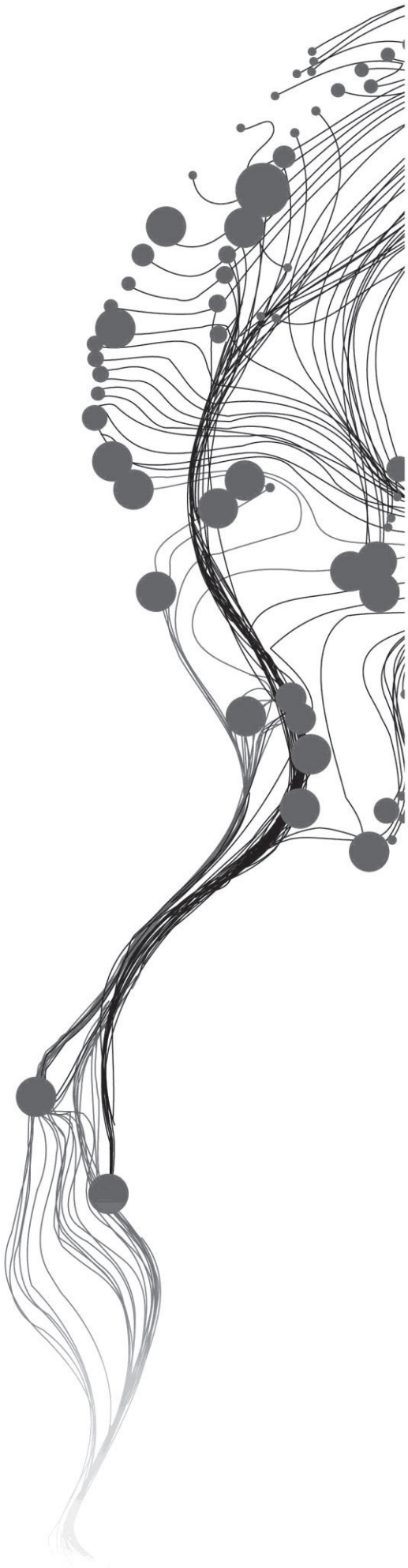

CLASSIFICATION OF DAMAGED BUILDINGS IN AERIAL OBLIQUE IMAGES AND LASER SCANNING DATA

OGUT JOSEPH CYPRIAN

Enschede, The Netherlands, February, 2013

Thesis submitted to the Faculty of Geo-Information Science and Earth Observation of the University of Twente in partial fulfilment of the requirements for the degree of Master of Science in Geo-information Science and Earth Observation.
Specialization: Geoinformatics

SUPERVISORS:
Dr. M. Gerke
Dr. K. Khoshelham

THESIS ASSESSMENT BOARD:
Prof. Dr. Ir. M. G. Vosselman (Chair)
Dr. N. Kerle, University of Twente (External Examiner)

ABSTRACT

The purpose of this research is to classify damaged buildings on an earthquake affected site based on some of the damage classes defined in the damage catalogue. This process of damage assessment is important as it facilitates planning for disaster response organisations. Knowledge on the state of the earthquake affected site comes from study of the data captured, which is representative of the site. Input for this research was in form of two point cloud datasets; an Aerial Laser Scanning and an Aerial Oblique Photography generated point cloud.

To gain an understanding of the nature of the two datasets a data analysis process was carried out. The process involved determining noise levels thus quality of the datasets. Successively, features defining unique properties of target objects of interest (i.e. walls, roofs, rubble and urban tree crowns) were determined and documented to ease in the classification process. This would help formulate the process of extracting target objects of interest.

The approach of classification here was a data driven, rule based classification process. This was informed by the ability of point cloud data to capture the true form of target objects individually, and status of the building environment collectively in an earthquake affected site. Subsequently a two step approach, involving classifying target objects of interest first before performing the overall building assessment to determine the damage class or type was followed. The method was developed on the premise that individual object properties cumulatively contribute to define the final damage status of any building.

The results of the classification process were then evaluated for completeness, correctness and quality to determine the success rate of the damage assessment process. This involved determination of the completeness, correctness and quality of the results using the true positive, false negative and false positive to compute the statistical values. It was found that the wall and roof classification results were relatively good, scoring 70's and 90's for completeness and correctness respectively. The rubble results were relatively low scoring high 60's in completeness and correctness respectively.

To conclude it all, the idea of combining two similar datasets to provide full coverage of the study area proved very successful. This presented a unique and innovative approach to capturing and analysing both vertical view or roof objects and horizontal view or facades of buildings within the dataset site. The classification process highlighted the feasible nature of combining ALS and AOP point cloud data to facilitate full site coverage, a feat extendible to any other target object of interest that is not related to the building environment.

ACKNOWLEDGEMENTS

My deepest gratitude goes to my supervisors Dr. M. Gerke and Dr. K. Khoshelham for guiding me through my Msc. Thesis. I am grateful for their understanding, patience, support and knowledge.

I would like to thank all the members of staff of the GFM department, Faculty of ITC, University of Twente, The Netherlands for their support that made me gain adequate knowledge to enable me pursue this Msc Degree and write the Msc. Thesis.

I would equally want to thank my friends and classmates for providing the mix of culture, experience and technical expertise that opened my understanding on working and teaming up with people from other corners of the globe.

My special appreciation goes to my family members for their continuous encouragement, guidance and support through all times, especially the hardest of all times.

Finally I dedicate my thesis to my parents A. W. Ogut and J. M. Ogut, my sisters, brother and my great pal B. J. Kemboi for the great assistance they offered to me during the entire period of this study.

TABLE OF CONTENTS

LIST OF FIGURES

LIST OF TABLES

LIST OF ABBREVIATIONS

2D	2 Dimensional
3D	3 Dimensional
ALS	Aerial Laser Scanning
AOP	Aerial Oblique Photography
CCD	Charge Coupled Devices
DEM	Digital Elevation Models
EMS	European Macroseismic Scale
ESE	East of South East
ExG	Excess Green index
FN	False Negative
FP	False Positive
GPS	Global Positioning Systems
GSD	Ground Sampling Distance
HRSI	High Resolution Satellite Imagery
INS	Inertial Navigation Systems
LiDAR	Light Detection And Ranging
NNE	North of North East
PCM	Point Cloud Mapper
pcl	Point Cloud Data
RANSAC	Random Sampling Consesus
RGB	Red Green Blue
SAR	Synthetic Aperture Radar
TP	True Positive
VHR	Very High Resolution

1. INTRODUCTION

Classification of damaged buildings is necessary for the rapid requirements of emergency response logistics on sites ravaged by disasters such as earthquakes. Geospatial techniques such as Aerial Oblique Photography (AOP) and Aerial Laser Scanning (ALS) provide fast means to capture site data for analysis on the devastation and loss experienced. Methods that ensure quick processing of this data to bring out the true picture are therefore of utmost importance.

Equally important is the extraction of entities that will help identify object classes of interest as roofs, walls and rubble that describe damaged buildings. Proper formulation of features, properties and processes that facilitate this is highly valuable. Hence the essences to identify and develop features that will help describe and extract the target object classes of interest within defined constraints, in this case being the threshold value of any feature that helps isolate any one target object of interest.

Furthermore, there exist established damage classes relevant for building damage assessment. There is thus need to identify entity feature combinations that help describe these damage classes and equally assist in identifying locations with the specific damage classes within the site of interest. Data acquisition on sites affected by disasters such as earthquakes occurs within reasonable time after the occurrence of the disaster. Depending on the target profession and techniques employed, the prevailing scenario of damaged structures is usually captured for later analysis and disaster response initiatives formulation. The scenario targeted in this research was that of an earthquake affected building damage site. Hence the aim of this research is to perform a classification of damaged buildings by defining rules to help extract target objects and practically define damage classes, based on which the assessment is implemented. This building damage assessment is based on point cloud data sourced from aerial laser scanning and aerial oblique photography.

1.1. Problem statement

The main problem is to identify and appropriately classify damaged buildings on an earthquake ravaged site based on point cloud data. Emphasis is on identifying and extracting entities relevant for defining objects cognisant with damaged buildings on an earthquake ravaged site and finding their unique features. The main task is to formulate feature attribute combinations that define a damaged building based on identified classes relevant for post earthquake point cloud data. This is succeeded by determining how to relate and cluster extracted entities to each pre earthquake existent building in order to define its damage class.

1.2. Motivation

Existing building damage documenting options such as the European Macro seismic scale (Grünthal, 1998) and the damage catalogue(Schweier & Markus, 2006) exposed the need to develop building damage ontology and classification that were relevant for geospatial approaches (Van Aardt et al., 2011) to building damage assessment. Further, due to site analysis capabilities based on point cloud data, the first motivation of this research is the need to formulate mechanisms to relate damage classes relevant to this data and formulate features that would enable defining of building damage based on the same data, limited to post earthquake information only.

Similarly, existing research had established knowledge on strengths exploitable to improve building damage assessment methods involving geospatial approaches. Emphasis on this involved combining the vertical advantage of aerial laser scanning with the lateral advantage of aerial oblique photography to capture the affected site, especially in bringing out the true form of the affected buildings on site. The second motivation for this research arises from the fact that the potential of point cloud data as input for extraction of entities that facilitate detection of buildings and related objects has been proven (Xu, Oude Elberink, & Vosselman, 2012) and was therefore worth exploiting to define damaged building parts and optimise research on effective building damage assessment.

In the ever modernising world, there is increased need for development of simpler and faster methods that facilitate use of available data. This is achievable via development and exploration of several guiding rules or constraints that may offer some beneficial degree of success. Hence the third motivation for this research is in exploring constraints usable to practically define damage classes and further perform the building damage classification based on the same.

Finally disasters keep on causing damage to property, both from time memorial through current times into the future. Their rising magnitudes as witnessed in the Haiti Earthquake of 12th January 2010 and the tsunami of Indonesia 26th December 2004, means more vast regions will be affected. The final motivation arises from two facts, the vast region data capture ability of geospatial data capture techniques and that buildings form a majority of structures constructed on the earth's surface hence any disaster, specifically earthquake hitting any part of the earth will actually affect them. This thus provides a push factor for research into methods that improve or develop and refine building damage assessment processes.

1.3. Research Objectives and Questions

The main objective of this research is to perform a classification of damaged buildings devastated by an earthquake. Focus was on analysing entities extracted from point clouds sourced from laser scan data and aerial oblique photographs. The research comprised of the following specific objectives and related research questions:

1. To identify building damage levels relevant for point cloud data.
    - What is the relevance of point cloud data for building damage classification?
    - How will damaged buildings be defined based on point cloud data?
2. To assess the effect of noise on point cloud data.
    - What is the level of noise in the input datasets?
    - How does noise influence the extraction of entities from point cloud data?
3. To identify characteristics of extracted entities usable in defining damage to a building.
    - What features of extracted entities are relevant for damage assessment?
    - How will the features be combined to define building damage categories?
4. To classify damaged buildings based on formulated damage levels.
    - How will the classification process be implemented?
    - What factors will affect the classification process?
5. To evaluate the results of the classification process.
    - How will the accuracy of the classification results be assessed?
    - What factors will affect the accuracy of the results?

1.4. Innovation

The innovative part of this research specifically entails use of combined input ALS and AOP point cloud data, and knowledge about damaged buildings on an earthquake affected site to perform building damage classification. Practically, it aims to take advantage of the complete coverage provided by the combined datasets to determine the overall damage classification process within defined constraints based on characteristics of extracted target objects.

1.5. Thesis Structure

This thesis consists of six chapters. Chapter 1 is the introduction and explains the problem statement, motivation, research questions and objectives, innovation and thesis structure. Chapter 2 is the literature review, followed by materials in chapter3 that gives an over view of data and software used in this research. Chapter 4 is data analysis that helps define and understand the input datasets. Chapter 5 explains the methodology; specifically the approach used in the damage assessment /classification process, and is succeeded by results and discussion in chapter 6. The final part in conclusion and recommendations is in chapter 7.

2. LITERATURE REVIEW

2.1. Introduction

Damage classification falls within the global action of damage assessment and mitigation, and is a key element of disaster response organisations. Disaster stricken localities experience huge losses as evidenced in the Haiti earthquake of 12th January 2010 (DEC, 2012), the Indonesian tsunami of 26th December 2004 (Hobart, 2012) and the Hurricane Katrina (NCDC, 2012). Damage assessment entails determining the losses experienced in any disaster ravaged region using varying methodology. It is executed based on data sourced from affected sites about damaged property due to the necessitated need for current damage assessment and future damage control.. The process has evolved over the years inclusive of its challenges and lessons (McEntire et al., 2012). From inaccurate data and information, through poor training and lack of preparedness to political and policy failures, the need for proper measures to facilitate appropriate response to disastrous aftermaths has developed and risen over time. The process ranges from data acquisition and processing, through target object extraction to the actual damage estimation or assessment and classification. The urge for more knowledge on damage assessment, associated data processing and mitigation measures has provided a push factor for more research into this area.

2.2. Data Acquisition and Processing

Accurate acquisition of information about any disaster ravaged site is of utmost importance. The prompt requirement of disaster response teams creates a need for quick data capture and processing mechanisms. Satellite imagery provides one option for quick capture of building data. However, given that even at 0.5m GSD per building damage assessment is still a challenge then Airborne data with higher resolution of about 17cm is then preferred (Gerke & Kerle, 2011). This can be sourced from Airborne LiDAR (Light Detection and Ranging) Scanning systems that facilitate quick provision of accurate geo-information for disaster management (Firchau & Wiechert, 2005). Further enhancement is by use of Aerial Oblique Photography to bridge the horizontal view not captured through the natural vertical view of Airborne LiDAR scanning systems. Aerial Laser Scanning and Aerial Oblique Photography provide fast means of data capture of any disaster ravaged site.

2.2.1. Aerial Laser Scanning

Aerial Laser Scanning entails application of LiDAR technology to capture 3D point data of the earth surface. The process includes varying scanning mechanisms, integration with GPS (Global Positioning Systems) and INS (Inertial Navigation Systems) systems, data processing and extraction of target objects as explained in (Vosselman & Maas, 2010). Key processes include Filtering (Sithole & Vosselman, 2005) that may involve use of filters that have varying capabilities (Sithole & Vosselman, 2004) to separate terrain from non terrain points, Segmentation (Sithole, 2004) and clustering that groups data based on identified criteria and classification that facilitates identification of target objects of interest (Vosselman, 2009). Its ability to capture object positional information accurately and fast provides an impetus for its use in portrayal of any disaster ravaged site.

2.2.2. Aerial Oblique Photography

This involves capturing of the terrain surface using aerial digital cameras mounted on mobile platforms at non vertical positions (Karbø & Schroth, 2009). The technology is enhanced by the development of

modern couple charged devices (CCD) arrays, multi-lens cameras and multi-head cameras. Internal and external orientation (Grussenmeyer & Al Khalil, 2002) of acquired images facilitates model scene development from which dense image matching techniques as semi-global matching and Patch-based Multi-View Stereo (Furukawa & Ponce, 2010) are applied to generate point cloud data (Gerke, 2009). Given the complex nature of urban scenes, use of aerial oblique photography provides a means for detailed and quick all round data capture of such areas especially building facades, a scenario targeted by this research.

2.3. Building Detection and Extraction

Buildings form a majority of structures constructed and therefore are always affected by earthly calamities such as earthquakes. Building damage assessment operations require their accurate capture and extraction from relevant data. First building objects are separated from other objects depending on the data in use. The next step entails outlining of building foot prints that are useful especially for two dimensional (2D) representations of buildings. Finally reconstructive modelling may be applied using topology to build boundary representation or using volumetric primitives to obtain a representative building model. Buildings, especially intact buildings may be detected and extracted from aerial images (Sirmacek & Unsalan, 2008), laser scanning data (Morgan, 1999), fusion of airborne laser scanner data and multi-spectral images (Rottensteiner et al., 2007), high resolution satellite imagery through object based determination of building foot prints (Vu, 2011), use of grey-value and gradient orientation (Sumer & Turker, 2005) and oblique airborne imagery based on robust façade detection (Xiao, Gerke, & Vosselman, 2012). Given the need to identify realistic 3D representation of buildings, Aerial Oblique Photography and Aerial Laser Scanning are preferred due to their geometrical and positional strength to depict the external form (walls and roofs) of buildings. The building detection process is then succeeded by damage definition and identification to enable determination of the damage experienced.

2.4. General Damage Classification

Damage classification and assessment varies depending on the cause of the damage, methodology employed and input information to be used. Majorly, it's implemented in relation to the key phenomena experienced in moments around the time a particular structure or building or target object was damaged. Practically, it's usually linked to the main causal phenomena from flood damage assessment (Qi & Altinakar, 2011), through hurricane damage assessment (Pistrika & Jonkman, 2010), wind damage assessment (Nateghi-A, 1996), and earthquake damage assessment (Oliveira & Campos-Costa, 2006) amongst others. The main urge is usually to create and disseminate accurate and updated information to the responsible disaster management organisations and authorities. Damage classification and assessment processes usually target specific objects of interest both natural and manmade. For this study, buildings were the target object of interest for study as they form majority of structures affected on most earthquake affected built environments.

2.5. Building Damage Classes

Depending on the approach to building damage classification, there exist several Building Damage Classification classes and types. The focus is mainly on earthquake related building damage. Amongst some of these are the Damage catalogue (Schweier & Markus, 2006) and the European Macro-seismic Scale (EMS–98) (Grünthal, 1998).

2.5.1. Damage catalogue

The damage catalogue defines building damage based on typical geometrical features of each damage type or class. Typical features used include total height difference to initial height, building volume reduction, surface structure, inclination change and debris size (Schweier & Markus, 2006). The main classes defined here are inclined layers inclusive of inclined plane, multi layer collapse and outspread multi layer collapse, pancake collapse inclusive of pancake collapse one storey and pancake collapse multi storey, debris heaps inclusive of heap of debris on uncollapsed storeys, heap of debris on vertical elements and heap of debris with plates, overturn collapse inclusive of overturn collapse separated, inclination and overturn collapse, and finally overhanging elements, all as illustrated in figure 2-1 below.

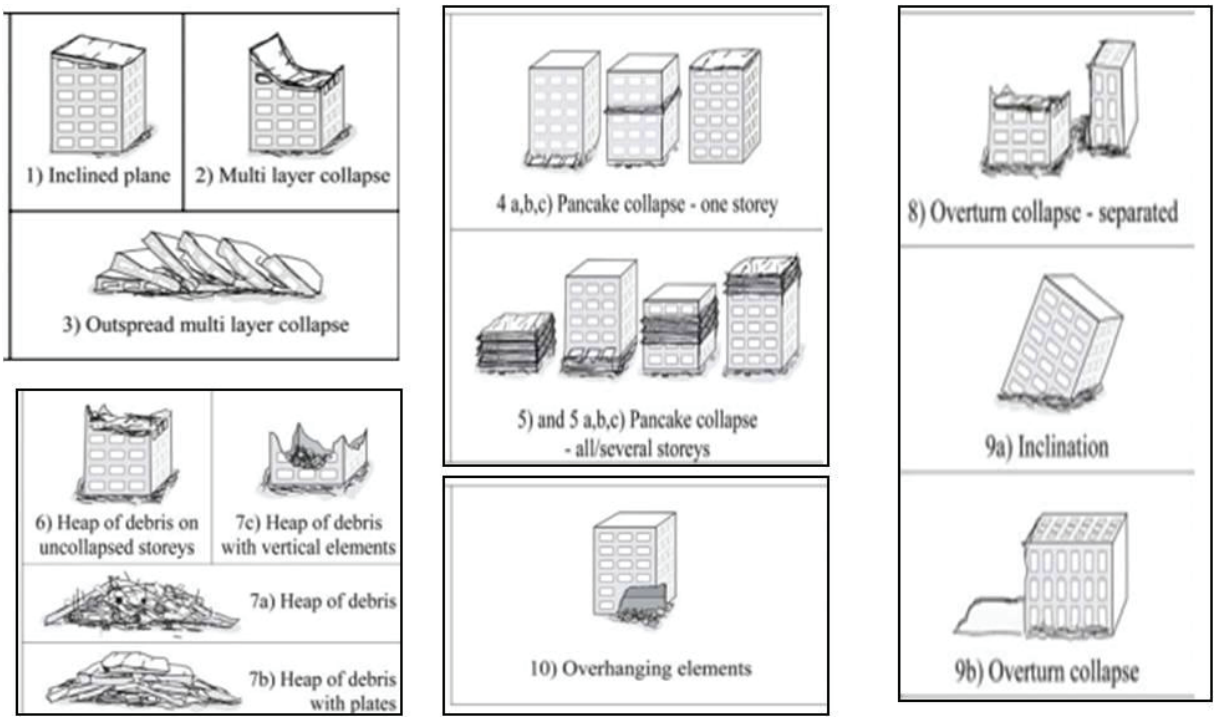

Figure 2-1. Damage classes defined on the Damage catalogue Source: (Schweier & Markus, 2006).

2.5.2. The European Macroseismic Scale (EMS-98)

The EMS–98 considers macro-seismic intensity in its classification of building damage. Buildings are classified by their key construction component as masonry, reinforced concrete, steel and wood from where specific grades relating to each class are defined based on level of destructive force and damage experienced. For masonry and reinforced concrete buildings the identified damage classes range from grade 1 to grade 5, respectively termed as negligible to slight damage, moderate damage, substantial to heavy damage, very heavy damage and destruction.

Building damage classification varies depending on the approach and scale of the process. It may be carried on site manual building inspection for the civil engineering and architectural approach or via a mapping approach that entails application of geospatial data capture techniques especially for vast ravaged sites.

The final approach, whether architectural, civil and structural engineering or geospatial approach to building damage assessment depends on the professional subject of interest. Architectural, Civil and Structural engineering approaches tend to encompass detailed individual onsite building damage assessment. They focus on close study of key building parts as walls, roofs and columns, mostly close on

building observations. Geospatial approaches tend to cover large scale site wide areas, using offsite assessment techniques and were proved successful during the Haiti earthquake disaster response activities (Van Aardt et al., 2011). The interest of this study was to perform a site wide general external building damage assessment; therefore the geospatial approach to earthquake affected building damage assessment approach was followed.

2.6. Eartquake Building Damage Assessment.

Earthquake building damage assessment using geospatial approaches has been researched upon and implemented using various input data and methodology. Geospatial approaches in this case referring to methodology for capture, processing and use of geo-data such as earth satellite imagery or point cloud data or earth's aerial photographs to solve geo /earth related problems. One approach involved the use of aerial photographs to assess damaged buildings after the 1995 Kobe Earthquake (Ogawa & Yamazaki, 1999). It involved manual human identification of damaged buildings via single photo or stereoscopic photo interpretation. More success was on wooden buildings and less on non wooden buildings that had less clear texture making it hard for human interpretation. The main problem was the variation in human interpreting ability that raised the need for automation. Furthermore geometry though visualized via stereoscopy was not exploited to enhance the true position of objects, specifically onsite buildings.

Progressive improvement came with the use of digital aerial photographs during damage classification after the 2003 Bam city earthquake in Iran (Rezaeian & Gruen, 2007). This involved automatic creation of digital surface models based on stereoscopy using pre and post earthquake imagery. Pre and post earthquake data was then compared to define damage to buildings as total collapse, partial collapse and no collapse, categories that still needed improvement to endear their relevance to geospatial building damage assessment methods. Differing human interpretation ability was still a limiting factor here too, an indicator of the urge to develop an automated building damage classification process.

Satellite imaging developments further improved building damage classification, as evidenced by incorporation of Landsat imagery for damage assessment after the 2001 Gujarati earthquake in India (Yusuf, Matsuoka, & Yamazaki, 2001). Optical remote sensing was applied in analysis of optical images with panchromatic bands sourced from Landsat-7 satellites. The basis was to check for significant changes in reflectance values after the earthquake. Differences in optical sensor values between pre and post earthquake satellite images were used to identify affected regions. Emphasis was on detecting affected areas and not actual variation of damage encountered on the identified sites. Dependency on pre earthquake information was also a key weakness.

High Resolution Satellite Imagery (HRSI) was used in damage detection after the 2008 Wenchuan earthquake (Tong et al., 2012). Pre and post seismic IKONOS image stereo pairs were used to determine 3D geometric changes by calculating difference between pre and post seismic digital elevation models (DEMS). Pre and post earthquake difference in building geometry was used to classify the damage as totally collapsed, partially collapsed and not collapsed. Though categorisation was done here, it was in a manner not fully relevant to building damage classification and geospatial sciences.
Similarly, ADS 40 images were acquired and used in identifying collapsed buildings in Wenchuan (Guo et al., 2009). Grey scale morphology was used to detect areas having collapsed buildings. Difficulties were experienced here in differentiating concrete bridges, rolling rocks and gravel from collapsed buildings. Further the process did not categorise specific damage to identified damaged buildings.

The need for proper categorisation led to documentation of damage classes in form of a damage catalogue (Schweier & Markus, 2006). Different post earthquake damage types for whole buildings were composed. This involved compilation of typical damage types of collapsed buildings into one damage catalogue. It was implemented by looking into the characterisation of affected buildings based on their geometrical features. This process enlightened the need for categorisation of building damage, and exposed the urge for further development or selection of damage levels relevant for geospatial science, and in this case relevant for point cloud data. However, despite having some relevant building damage classes for geospatial data, specifically point cloud, successive damage classification processes have not employed the developed damage catalogue classes in the output of their results.

Damage classification incorporating LiDAR (Light Detection and Ranging) was done as depicted in (Oude Elberink et al., 2011). This approach was aimed at detection of collapsed buildings and did not progress into categorising them. Rule based classification was applied using appropriate combination of identified attribute values to detect collapsed buildings. The process did not exploit the geometrical strength of LiDAR to depict building geometry. An extension into this would have enabled categorisation, especially involving the damage catalogue classes, a step that this research moved in to exploit.

Further efforts used high resolution aerial oblique imagery to determine the structural seismic damage of buildings (Gerke & Kerle, 2011). Imagery from Pictometry inc. was used as input into this process. Despite incorporating oblique aerial imagery that possessed the ability to enable in-depth façade detection and analysis, formulated classes were limited to intact roof, damaged roof and facades. The detectable classes would have been improved on to conform to some of the achievable damage classes as defined in the damage catalogue. Further this process incorporated part of the European Macro Seismic Scale classification into its final assessment rules despite recognition of the fact that these classes were not entirely suitable for classification of individual damaged buildings based on geospatial techniques.

Multi- imagery has also been employed for building damage classification via use of Multi-Mutual Information (MMI) to perform post earthquake building damage assessment (Tian-Lin & Ya-Qiu, 2012). It involved use of pre event optical images and post event SAR (Synthetic Aperture Radar) images to determine pre earthquake and post earthquake building status. Pre earthquake building geometry from the optical images is compared with modelled rectangular objects from post event SAR images in a similarity analysis to determine the damaged and non damaged buildings extended into collapsed, subsided and deformed status. This process still didn't have well defined damage classes as defined in the damage catalogue and also required quite some input of pre earthquake data. A similar approach involved the use of pre event VHR (Very High Resolution) optical and post event detected VHR SAR imagery to obtain building footprints from which similarity analysis was done to determine damage status of a building (Brunner, Lemoine, & Bruzzone, 2010). High similarity was taken as a signature for being intact while low similarity indicated some damage. This approach still depended on pre earthquake information and did not categorise damage to more specific damage classes.

Multi-sensor imagery approach was also used in building damage assessment and mapping (Lodhi, 2013). This approach involved input of Advanced Land Imager (ALI) imagery and Hyperion imagery to identify damaged buildings and spectral signatures of objects of interest respectively. The process involved manual identification of clusters of interest, manual delineation and digitizing of raster polygon areas of interest and classification of objects into damaged buildings, intact buildings and vegetation. This approach did not exploit usable classes based on the damage catalogue and still had vast dependency on manual intervention. This process was pixel based thus it could not bring out the building geometry status, a key component that solidifies use of point cloud data in defining building damage status. Further the process

was affected by spectral similarities of rubble and crumbled building, and barren land creating considerable spectral confusion which would easily be differentiated via the 3D capability of point cloud data.

Simulation has also been employed to assist in building damage assessment. This involved creation of pre and post earthquake building models to facilitate change detection and subsequent building damage identification, assessment and classification (Schweier, Markus, & Steinle, 2004). This process though effective has high dependency on pre earthquake information and further formed models may not actually represent the true status of target buildings. Direct use of 3d form of point cloud data of an earthquake ravaged site tends to depict a better realistic state of buildings on an earthquake ravaged site. Automated assessment of post earthquake building damage has also been implemented based signature from geospatial data (Dong & Guo, 2011). This approach involved 3 Dimensional Triangulated Irregular Network (3D TIN) densification followed by 3D shape signature analysis. It limited its search to four target models which would not fit into the multiple natures of real world buildings. Further the process was equally dependant on pre earthquake data and damage was only detected but not classified into specific identifiable categories.

Building damage assessment is evidently an area of great interest given the increased research output in relation to the same. Successive geospatial approaches have employed use varying data and methodology to achieve a specific objective in relation to building damage assessment. With increasing success, from multi-spectral images that were used to differentiate damaged and non damaged areas, through aerial photography that facilitated improved categorisation of the damage to laser technology that helped specifically identify target building parts, the urge for better recognised building damage classification has risen on. However, despite recognition of the viability of categorisation of building damage as exemplified in the damage catalogue, the same is not employed in the final output of most building damage assessment processes. Further, efforts to assess building damage on earthquake affected sites have majorly concentrated on damage detection, without extending organisation of their results into recognised damage classes. The results are mostly presented in user defined classes, majorly convenient for their output. This provided an impetus for this research to try and categorise the output of its classification process in line with definable damage classes based on the damage catalogue.

Further, building data capture and representation in 3D tends to capture most detail of any site of interest dominated by building structures. Data capture techniques that have the ability to capture this detail are therefore of utmost importance. Aerial Laser Scanning and Oblique Aerial Photography possess this ability of capturing building information in 3D.This ability presented in the vertical and lateral advantage of LiDAR and Aerial Oblique Photography generated point cloud data, enables capture and provision of complete building external form, a great feat targeted for exploitation by this research. Moreover buildings can be disintegrated into several recognisable parts majorly roofs and walls. This is encouraged by the fact that building construction is a result of assembly and erection of several minor structural parts. Such structures are easily captured in segment form based on point cloud data. The segmented parts are then exploitable for damage analysis as targeted by this research, based on which the final damage type or class is defined. This helps build up an inclusive all round picture of any particular earthquake damaged building.

Given the form and structure of building parts can be stated within set constraints, walls being upright and roofs being above walls amongst others then the same can be extended during building damage assessment. Further, the same constraints are practically applicable in defining damaged building parts and the overall building damage status within the site of interest. Extending this approach formed the guiding factor in using the rule based approach to perform the damage classification within this research.

3. MATERIALS

Material input for this research was in form of two point cloud datasets and software. The datasets were LiDAR generated point cloud and Aerial Oblique Photography generated point cloud. The software used were Point Cloud Mapper and Matlab. The use of point cloud data was preferred upon as it ensured adequate capture of the geometric form and structure of the buildings which were the main target objects of this research. For proper classification of the damaged buildings, it was necessary to be able to identify key components of building structures. This was in form of planar segments and clustered points that were generated due to the positional capability of the point cloud data. Further adequate processing and visualization of the input data was facilitated by the use of functioning software, in this case the PCM and Matlab. The software enabled the filtering, segmentation, clustering, visualization and cropping of the point cloud datasets, and basic implementation of the proposed classification.

3.1. Datasets.

3.1.1. LiDAR point cloud dataset (LiDAR pcl).

This was acquired by Kucera International between January 21-27, 2010 using a Leica ALS50 LiDAR system. This was done as part of the damage assessment efforts during the evaluation of effects of the earthquake that hit Haiti on the 12th of January 2010. It has an average point density of about 3 points per square metre (3.4 pts/m2) (SDSC, 2012). This dataset contains intensity, specifically reflectance information which was acquired as a result of the LiDAR system in use that possessed the ability to record the return amplitude of the received echo. Specifically the dataset in use covers the north western part of the Port-au-Prince area. Figure below shows the dataset visualized using PCM software and potrayed by reflectance values.

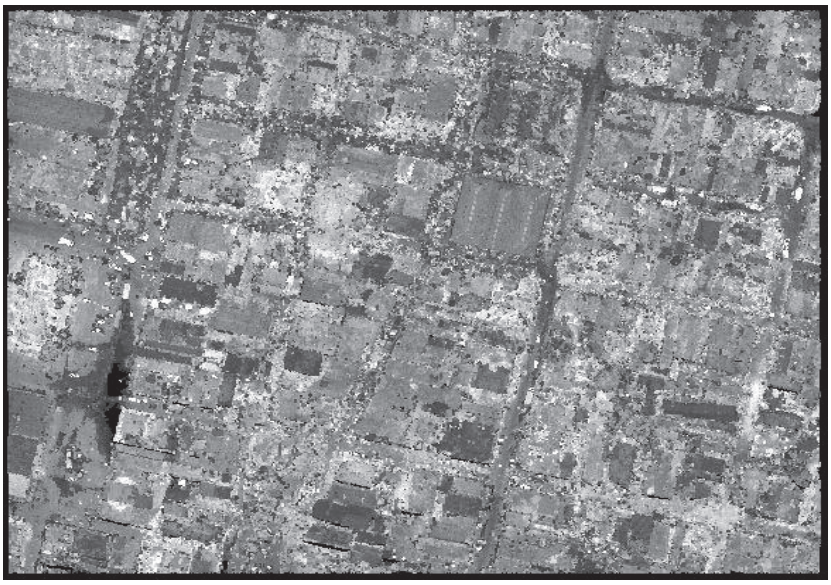

Figure 3-1. LiDAR point cloud visualized using reflectance.

3.1.2. Aerial Oblique Photography point cloud dataset (AOP pcl).

Aerial oblique imagery acquired by Pictometry inc. above the Port-au-Prince area after the Haiti earthquake of 12th January 2010 were used to generate point cloud data. The images were acquired at a height of 1000m above the ground using cameras that captured both forward, backward and side views, a feat that enabled capture of the facade of buildings. The arerial oblique images were then processed for

camera calibration and orientation. Further, common areas on non damaged building areas were identified on both the images and the LiDAR point cloud, out of which the latter's coordinate information, was extracted and used to geo-reference the aerial oblique images. Given most areas were covered by a minimum of two images, stereo overlaps were exploited for dense image matching. Patch-based Multi View Stereo (PMVS) dense image matching technique was then employed to derive point cloud data (Furukawa & Ponce, 2010). It involved identification of salient points on as many stereo pairs as possible. Epipolar constraint was applied to limit the search space and hasten the matching process. Initial identified 3D points were taken as patch candidates were triangulated upon to develop bigger patches. However, wrong matches were filtered by applying heuristic methods beyond which the remaining patches were optimized upon via the discrepancy minimization procedure. To densify the patches, the process was iteratively implemented during the patch expansion and filtering stage. The result was a collection of patches of points that contained additional building façade and colour information, the Aerial Oblique Photography generated point cloud dataset (AOP pcl). These dataset provided additional façade information and natural colour information. Figure 3-2 below shows the AOP pcl dataset visualized using PCM software and potrayed by colour information (RGB values).

Figure 3-2. Aerial Oblique Photograph generated point cloud visualized using own colour.

3.2. Software

These were the tools used to gain an understanding of the datasets used and also process them as deemed. The software used were PCM[1], Matlab[2] and Quantum GIS. PCM was used for point cloud processing, specifically filtering, segmentation, visualization, cropping and conversion of format. Matlab was used mainly for the implementation of the proposed classification process in form of a basic algorithm. Quantum GIS was used to prepare the final maps of the classification result.

[1] Developed by Prof. George Vosselman of The Earth Observation and Science department, Faculty of ITC, University of Twente.
[2] Matlab version 7.9.0.529 (R2009b)

4. DATA ANALYSIS

Data Analysis was performed to help in the understanding of the input datasets and characteristics of target objects (walls, roofs, rubble and vegetation). Specifically it involved visualizing the dataset information, performing noise level analysis, determining target object characteristics, features analysis and entity extraction, and determining damage types definable based on the damage catalogue. The result was an understanding of the dataset, the scenario of the site of interest and identification of features defining target objects of interest.

4.1. Dataset Visualization

Dataset visualization was performed using PCM software in order to gain a visual appeal of the datasets (LiDAR point cloud and an Oblique image generated point cloud). They were visualised in reflectance, height colour and own colour using PCM software, as shown in figure 4-1. Reflectance and height colour was visualised based on the LiDAR dataset while the natural colour was visualised based on the AOP dataset.

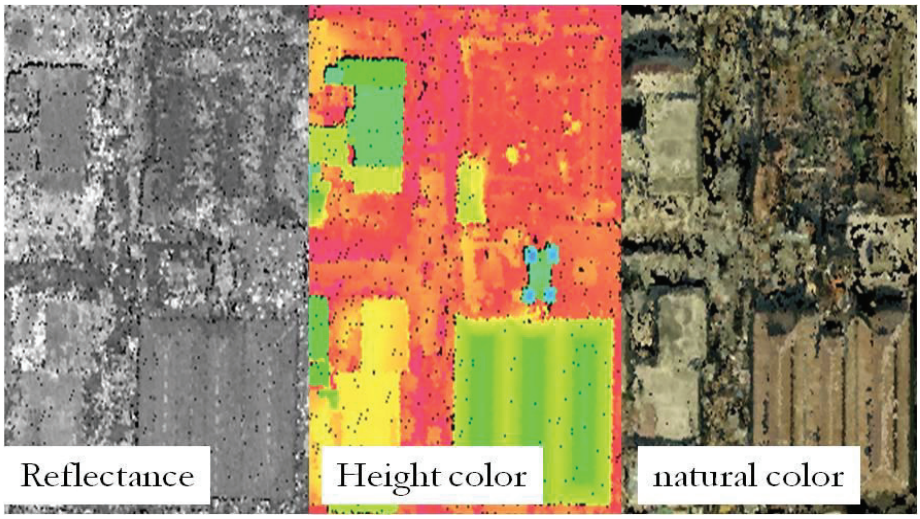

Figure 4-1Point cloud visualization using reflectance, height colour and natural colour.

The natural state of the datasets was captured and understood. Key observations noted here were;

1. Both datasets by virtue of point cloud nature contained positional information (3D coordinates) depicting object geometry, that was useful for wall and roof objects identification. Visually, walls appeared vertical and roofs appeared in horizontal and non –horizontal positions that were further away from the vertical.
2. The LiDAR datasets contained additional radiance information in form of characteristic object reflectance. This was found to appear more pronounced in areas that had partially or fully collapsed concrete building structures.
3. The aerial oblique imagery generated point cloud contained additional colour information (RGB values) that formed a useful visual link to the natural object status, especially the green nature of urban tree crowns.

This facilitated the ease of identifying target objects by visual appeal and identification all through reflectance, height colour and own natural colour.

4.2. Noise analysis

Given ideal conditions, point cloud data would form an exact fit of target surfaces. However, naturally the acquired point cloud data tends to have deviations off the target object surfaces.
Noise in this case was considered the amount by which point clouds deviate from an ideal fixed plane of the target object surface. Both LiDAR and AOP point cloud have varying causes of their noise levels. The automatic acquisition process of the LiDAR data during scanning with highly calibrated Laser Scan equipment gives it the added value of being more accurate hence less noisy. However, the AOP point cloud having been acquired via a combination of processes involving photograph orientation, through stereoscopy and dense image matching via patch-based multi view stereo carries within it cumulative errors from each stage. This leads the AOP point cloud to have higher noise levels as illustrated in figure 4-2 below. However given that AOP point cloud captures the horizontal facade view of buildings is not captured by vertical nature of Aerial LiDAR scanners, AOP input is considered valuable to ensure complete and representative data capture of target objects hence the trade off with its noise levels.

For this research, samples of same target objects from both datasets were extracted at various locations. Target objects of interest were walls and roofs, however due to the LiDAR data not capturing walls, the analysis was limited to roof plane surfaces. A plane fitting residual analysis in form of a Matlab code was implemented by applying the equation of the plane in 3D to determine the parameters of a fit plane defining each of the extracted roof plane segments. The implemented code incorporated Random Sampling Consensus (RANSAC) that ensured that the fitted planes were not influenced by outliers. This was due to RANSAC's conceptual simplicity and resilience to gross outliers in the data. This was useful as noise presence in the datasets indicated the likeliness of having outliers too within the dataset. Taking the LiDAR fit surface as the correct one, point offsets and standard deviations off this surface for both datasets were computed. The equation of a plane in 3D space is expressed below.

$$aX + bY + cZ + d = 0.$$

Where; a, b, c are the x, y, z components of the normal unit vector.
d is the perpendicular distance from the origin,
X, Y, Z refer to the 3D coordinates of any arbitrary point within the dataset.

The standard deviation of both datasets off the LiDAR fit surface was then calculated to determine the level of noise on each sample from the two datasets. This was done in by considering the LiDAR fit plane as being the true surface for both datasets. Further the mean offset of AOP datasets was computed off the LiDAR fit surface. The results in form of empirical standard deviation are as presented in tables 4-1.

standard deviation units (cm)

σ	Roof1	Roof2	Roof3	Roof4	Roof5	Roof6	Roof7	Roof8	Roof9	Roof10
LiDAR pcl	2.101	2.846	2.990	3.015	1.497	6.097	3.595	1.456	1.915	3.126
AOP pcl	10.074	14.401	13.835	25.512	11.036	15.529	9.803	22.368	8.758	13.373

Table 4-1. Standard deviations of samples of roof segments off the respective surface fit planes

The resultant fit planes from LiDAR point cloud were plotted against both respective AOP and LiDAR point cloud data for corresponding surfaces and visualised as illustrated in figures 4-2 and 4-3 below.
As observed, the LiDAR point cloud tended to be closer to the fit surface compared to the AOP point cloud. An indication of higher noise levels in the AOP point cloud compared to the LiDAR point cloud.

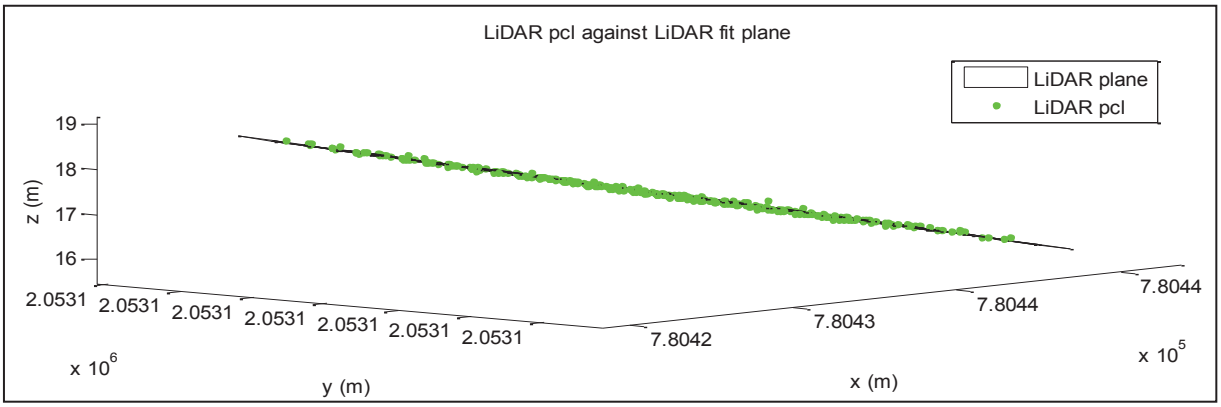

Figure 4-2. LiDAR point cloud fitted against LiDAR fit plane

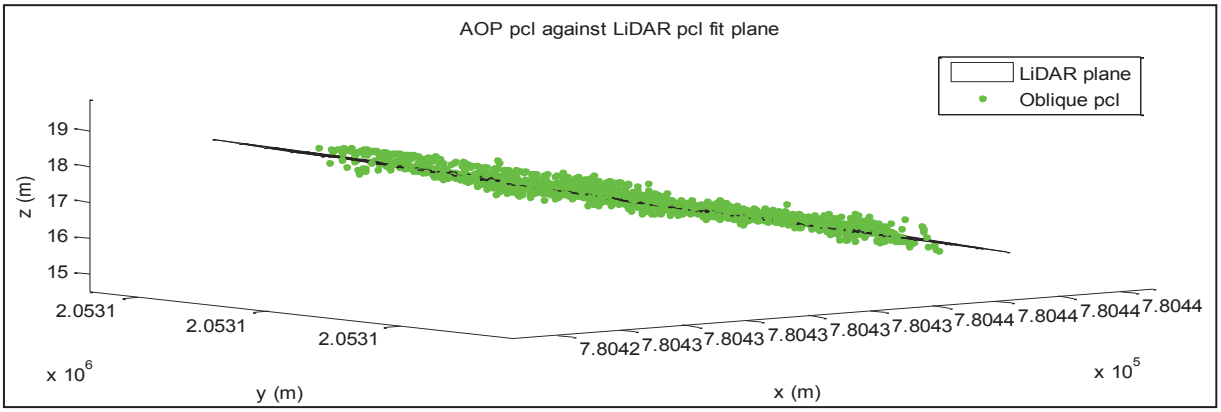

Figure 4-3. AOP point cloud fitted against LiDAR fit plane

Plots of the Gaussian distribution of the offsets were visualised as illustrated in figure 4-4 below. A key observation here was the sharp rise and narrow shape of the LiDAR point's offsets compared to the low and spread nature of the AOP point's offsets. This indicated closeness of the LiDAR points offsets to their mean as compared to the AOP point cloud, a pointer to lower noise levels in the LiDAR data compared to the AOP data.

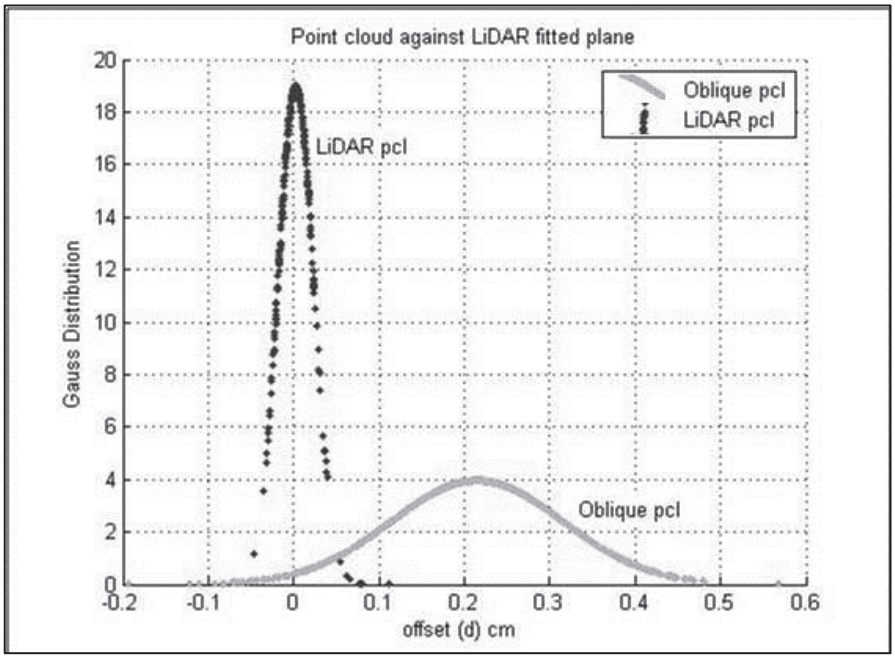

Figure 4-4. Gaussian distribution of offsets from LiDAR fit planes

The LiDAR point cloud had smaller empirical standard deviation values compared to the aerial oblique imagery point cloud, an indication that noise was higher in the Oblique point cloud in relation to the LiDAR fit surface.
Checks on parallelism of fitted planes from the same areas on both datasets involved comparing the inclination angles of flat roof samples as presented in table 4-2.

difference in	Roof6	Roof7	Roof9	Roof10	Roof11	Roof12	Roof13	Roof15	Roof16	Roof18
i_angle (˚)	0.080	0.506	0.487	1.049	0.825	0.672	0.958	0.326	0.272	2.570

Table 4-2. Inclination angle differences between pairs of flat roofs

It was expected that the difference between inclination angles for the same area fit planes from the two datasets would be zero. However, there were slight variations considered to have resulted from the different acquisition dates of the two datasets, the earthquake aftershocks that hit the site area and changes to the post earthquake structural status of the buildings. Significant variations would have occurred on areas where the existing structure on site had been extensively modified on site.

4.3. General dataset analysis

A general dataset analysis was carried out by comparing the mean offsets across the samples from various locations. This was due to the urge to detect the presence of any specific systematic tilt or site wide shift between the two datasets. The site of interest was divided into four regions; North West, North East, South West and South East from which the departures values from each region were plotted together and compared. As illustrated in figure 4-5 below, the offsets were found to have random variations with no tendency of being skewed in any direction.

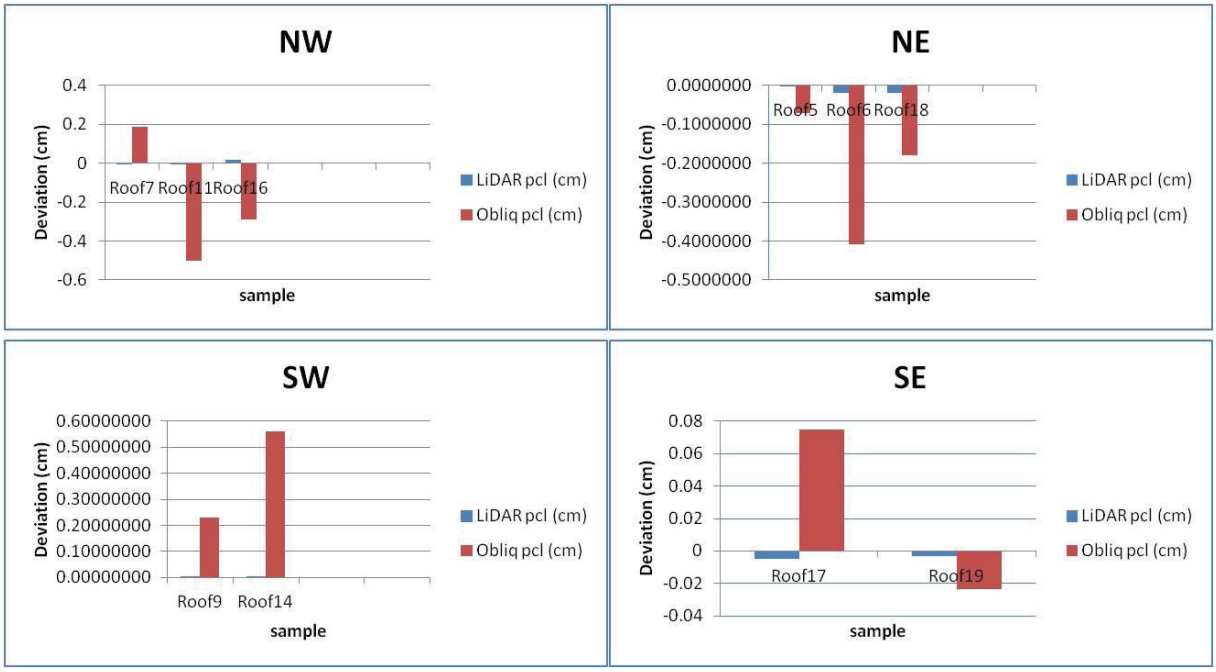

Figure 4-5. General Datasets offsets across the representative area.

4.4. Target object analysis

Target object analysis was implemented to facilitate identification of defining features for our target objects (walls, roofs, rubble and vegetation) based on manually extracted samples from both datasets. These objects were considered key to understanding the building environment in a typical built up site, hence key to defining the status of any earthquake affected building environment. Given the available information from the datasets was positional coordinates, colour and radiance (reflectance), defining characteristics were to be identified based on these.

4.4.1. Walls

By definition, these were vertical surfaces or near vertical surfaces that form the sides of buildings. Wall samples from the oblique image point cloud were analysed for unique characteristics. Using the plane fitting equation, the x, y and z components of the normal unit vector were computed. These were related by comparing them to the normal unit vector where the difference between the vertical and the vector in the direction of the plane is equated to the difference between the horizontal vector and the direction of the normal unit vector of the plane hence the adaptation of the equation as above. The inclination angle was then computed using an adopted formula indicated below and as illustrated in figure 4-6;

$$i = \theta = \cos^{-1}\left(\frac{a1 \cdot b1}{|a1||b1|}\right)$$

Where $\widehat{a1} = aX + bY$ is the horizontal vector and,

$\widehat{b1} = aX + bY + cZ$ is the normal unit vector of the plane.

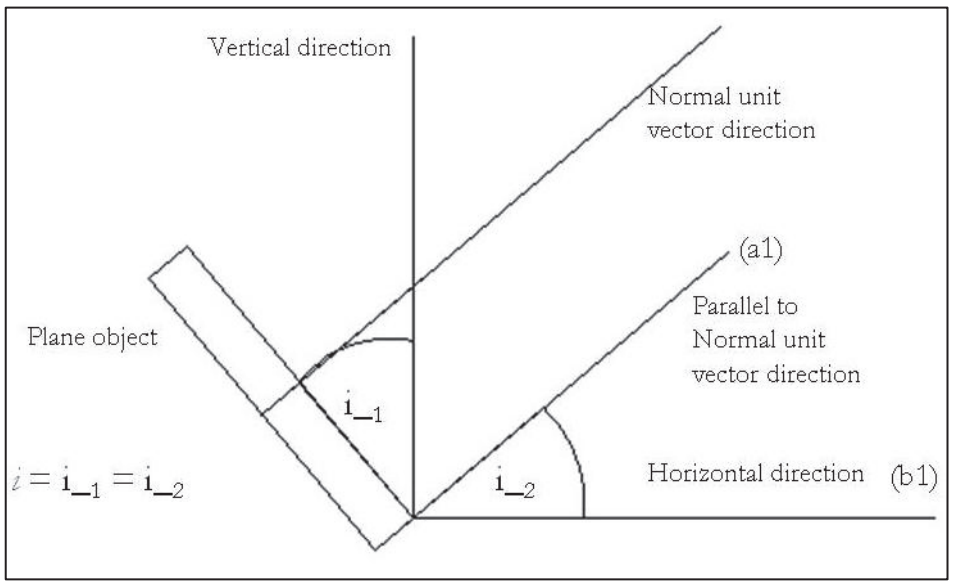

Figure 4-6. inclination angle based on normal unit vector

The z component of the normal vector, the inclination angles and the horizontal orientation for 17 wall samples were then computed. The results as illustrated in figure 4-7 below, are;

1. The z component of the normal vector was found to have values less than 0.3,
2. The inclination angles (i) were computed and found to have values falling below 20 degrees,
3. The horizontal orientation portrayed the horizontal directional set up of the buildings in two main bearings generalized as north of north east (NNE) and east of south east (ESE).

Despite correlation existing between the z component of the plane normal vector and the inclination angle, both were included as each had its unique role. The z component was deemed useful for differentiation of wall segments from the rest, however given wall damage included wall tilt

measurable by the inclination angle it was found necessary to have both. This is so as the research process not only aimed at detecting target objects but also determining their damage levels.

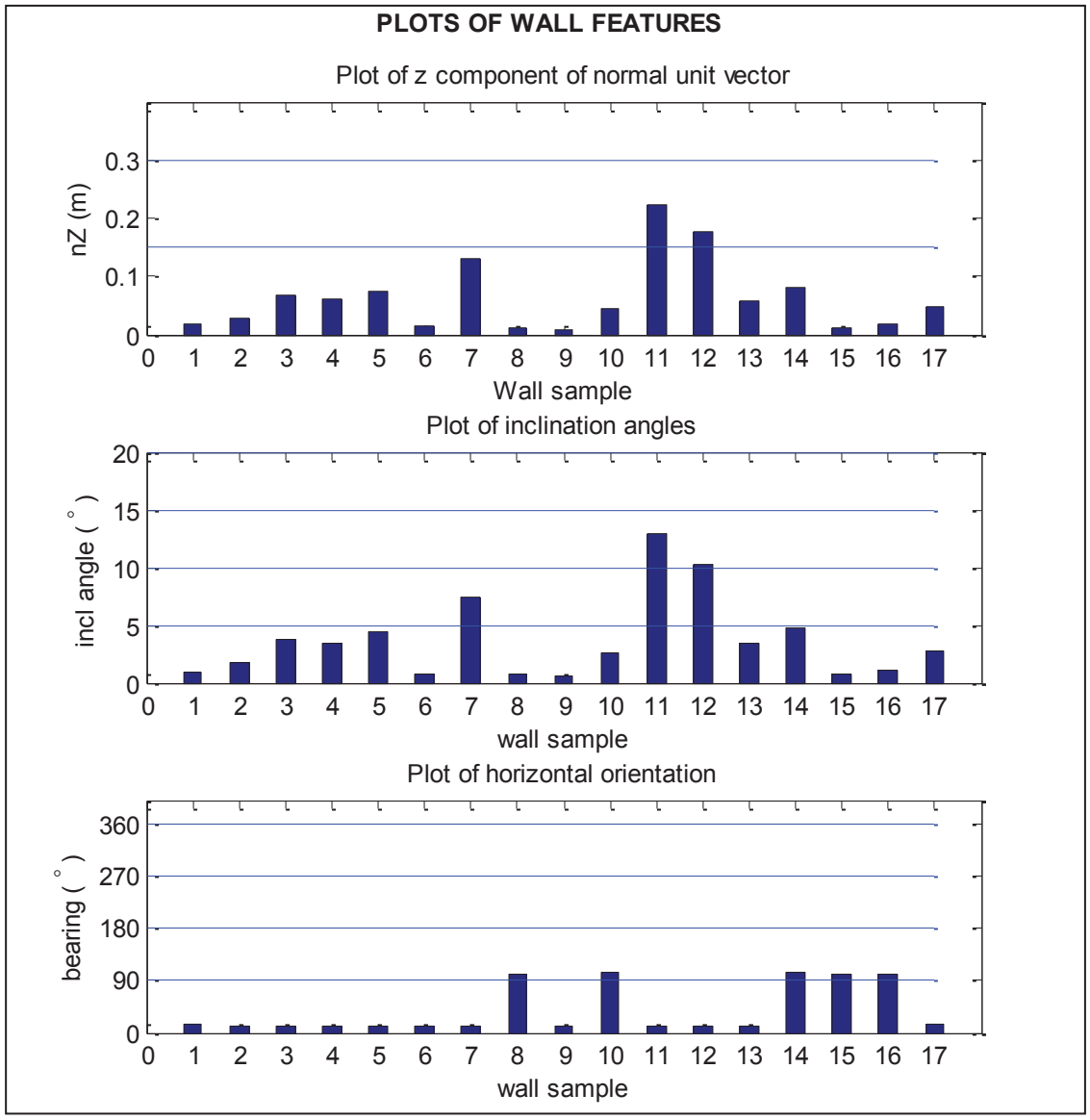

Figure 4-7. Wall samples plot of z component of normal vector, inclination angle and horizontal orientation.

4.4.2. Roofs

These were taken as structures forming the upper covering of buildings, their positional and size information was studied. Similar to walls, the plane fitting equation was used to determine the components of the normal unit vector of the roof planes. Inclination angles and horizontal orientation too were computed and observations noted. The observations as illustrated in figure 4-8 were;

1. The z component of the normal vector had values greater than 0.7,
2. The inclination angles were greater than 30°, in the range of 55 to 90 degrees,
3. The horizontal orientation varied widely from 15° to 293°.

They were equally found to have large segment sizes. Another key feature usable here was the inclination angle and orientation that was observed to be the similar for opposite pairs of gable roofs. The orientation was computed based on the x and y components of the normal unit vector.

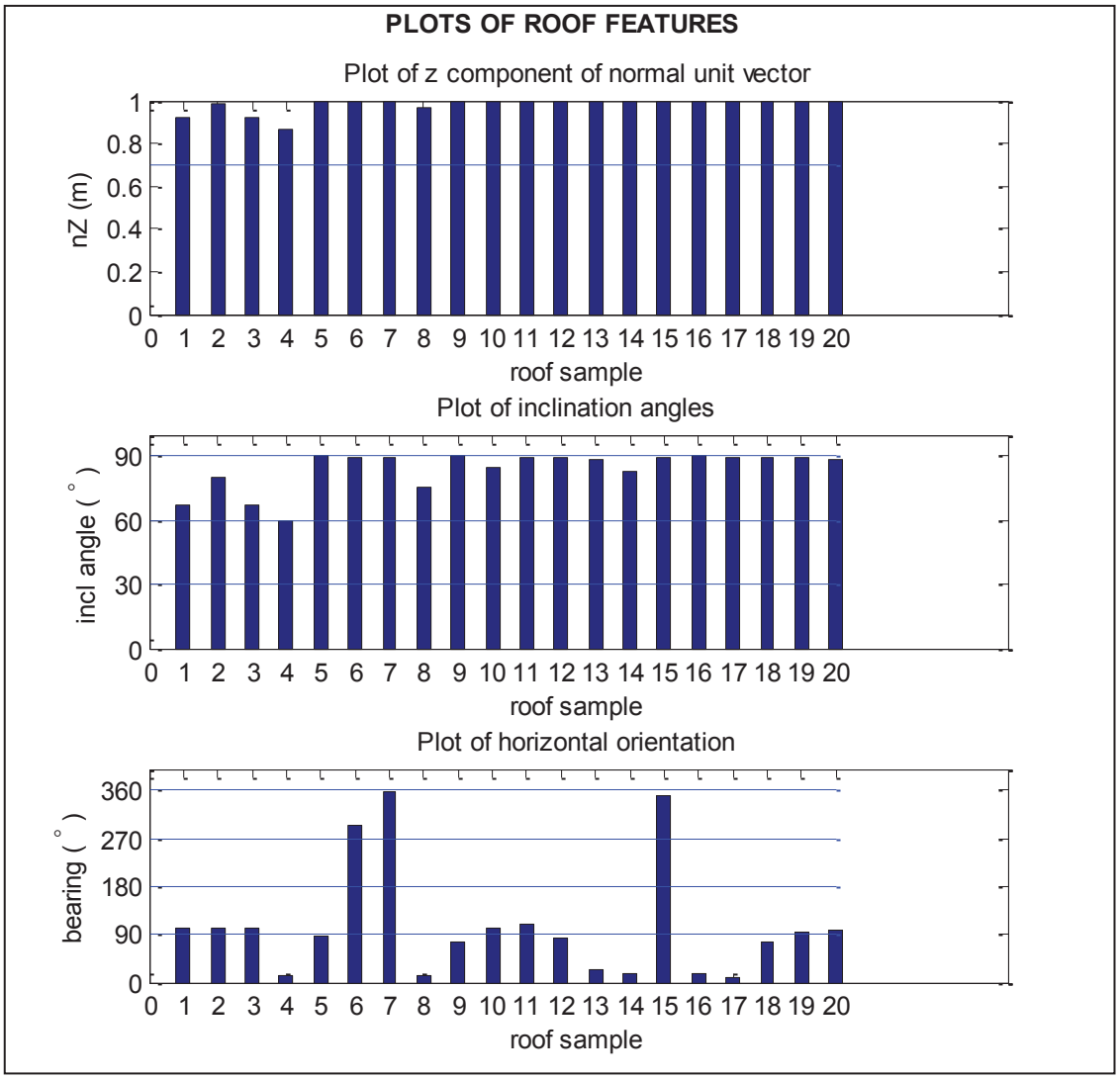

Figure 4-8. Roof samples plot of z component of normal vector, inclination angle and horizontal orientation.

4.4.3. Rubble (Debris)

Rubble was taken as broken pieces of collapsed walls and roofs, specifically of concrete structures. First the LiDAR point cloud was visualised using reflectance values, from where concrete rubble was noted to be more pronounced, and in natural colour the element of broken pieces was also seen as illustrated in figure 4-9. Several rubble samples were extracted and analysed for mean reflectance values and segmented size. Key observations noted as illustrated in figure 4-10 were;

1. The mean segment sizes generally fell below 20 points,
2. The mean reflectance values were mostly above 115.

The observations help form the rubble identification and extraction strategy where segmentation was carried out on the LiDAR dataset from which segments of size 20 or less were extracted. These were then clustered using the connected components functionality of PCM into groups of similar points. This was because the form of the rubble groups was best represented in clusters and not plane segments. Further,

given the close nature of rubble pieces, it was found that rubble sites had broken pieces of slightly larger segment size falling around the bright reflectance clusters hence consideration was given to these pieces for those that had segment sizes less than or equal to 60 points. This defined the rubble of this research as it occurred mostly around collapsed walls or columns or slab roofs

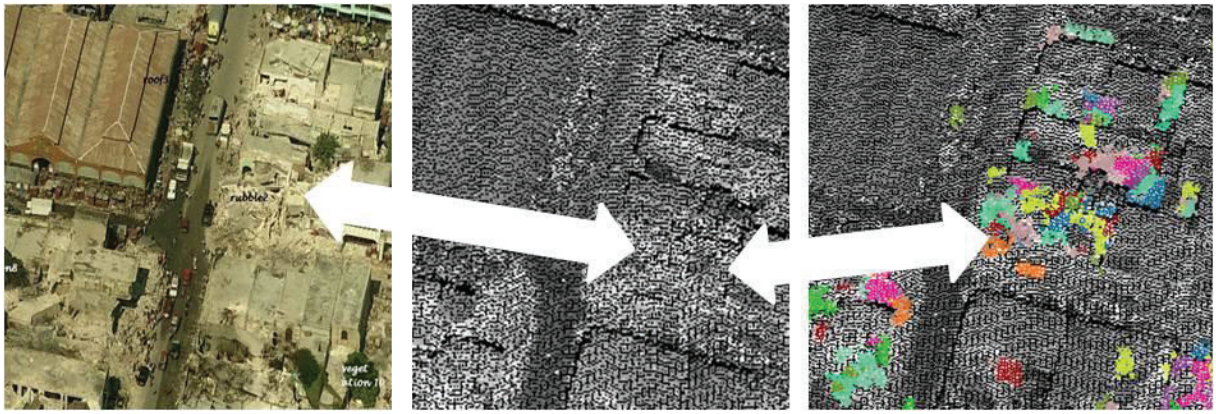

Figure 4-9. Rubble locations; natural colour, reflectance and selected rubble segments

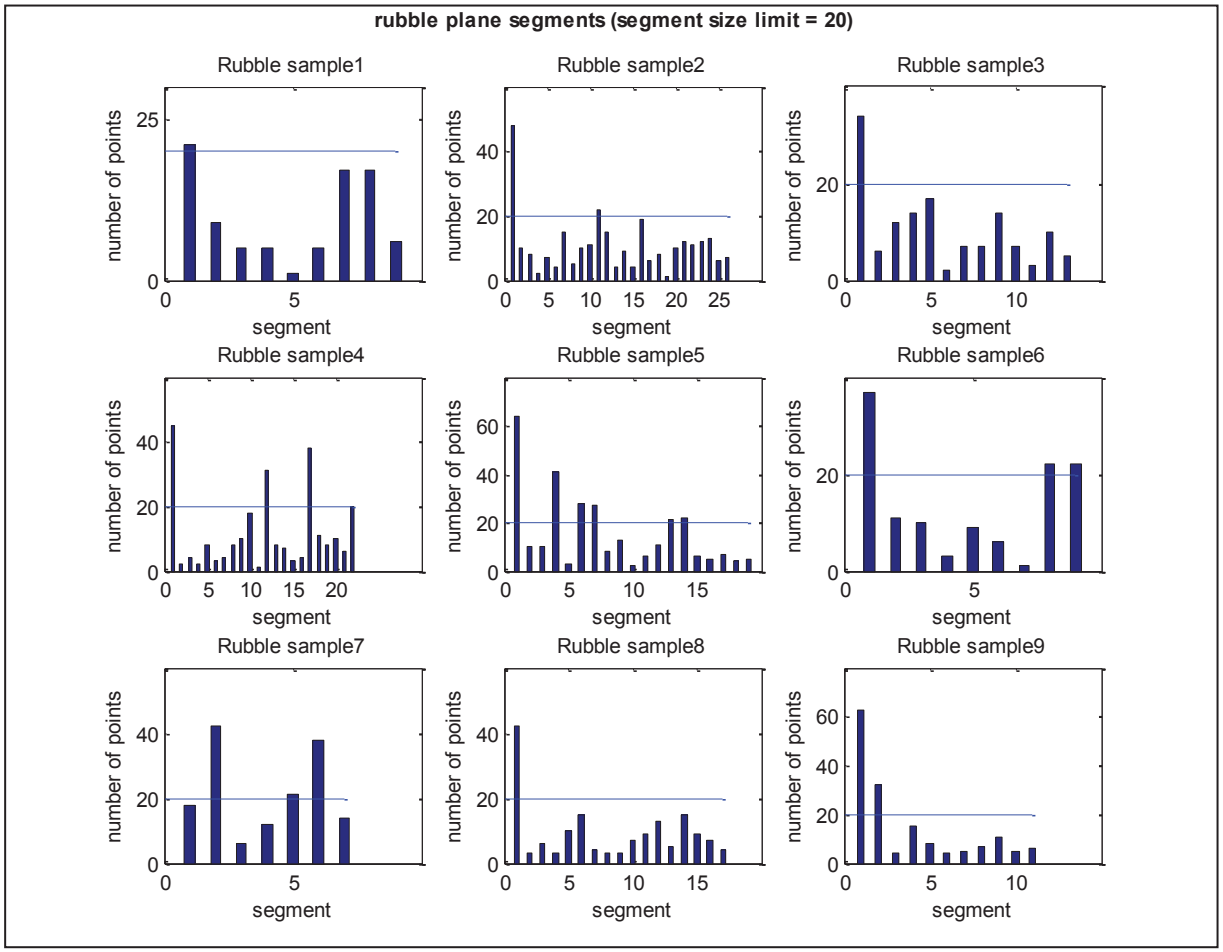

Figure 4-10. Plane segment sizes within rubble samples

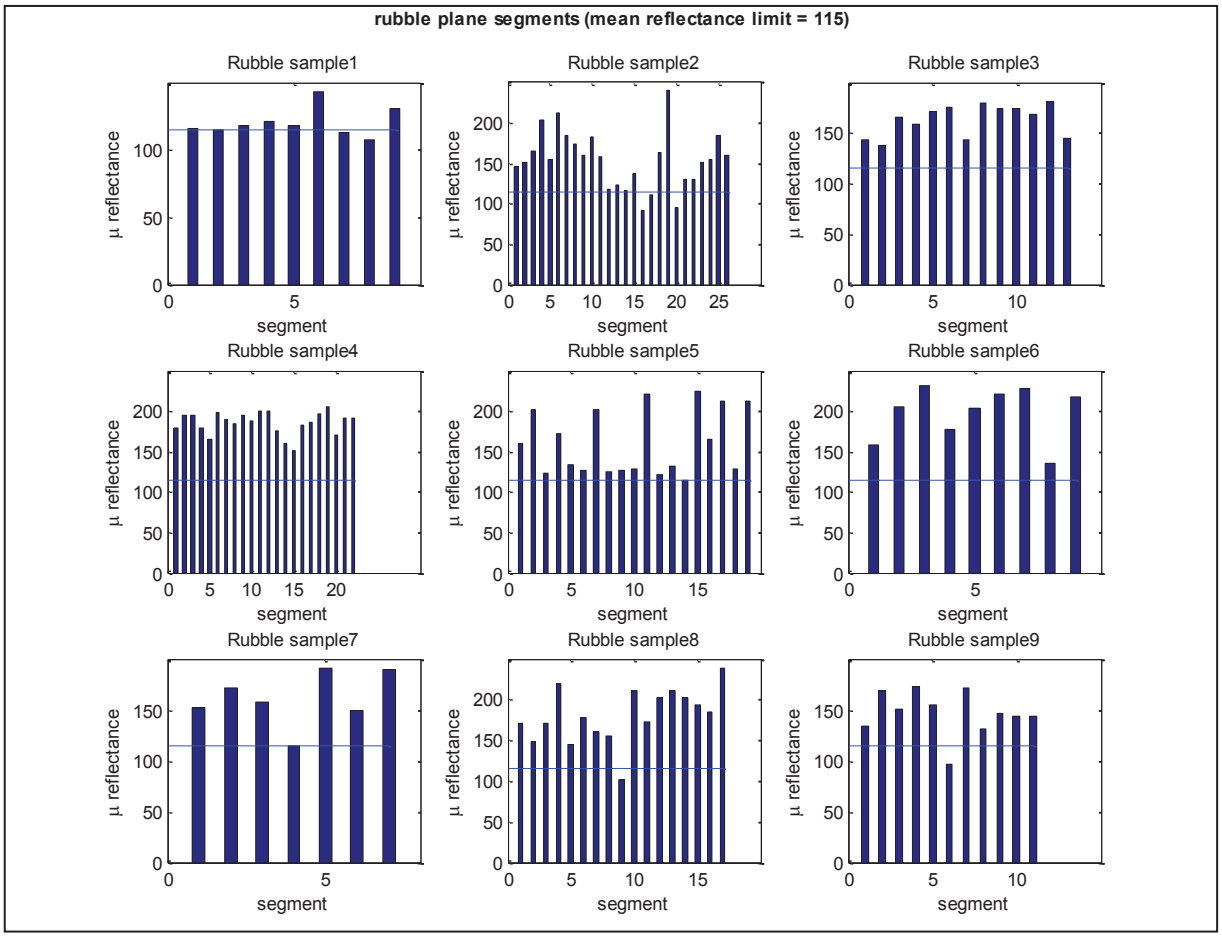

Figure 4-11. Plane segments mean reflectance within rubble samples

4.4.4. Urban tree crowns

Urban tree crown understanding from the visualization of the oblique datasets, tree crowns had dominant green colourations and tended to grow more vertically than horizontally. Tree crowns were identified based on colour information and form.

Tree crown samples were taken and analysed for green colour content based on mean green and excess green index, and crown base to height ratio using the crown segments standard deviations in x, y and z . The results as illustrated in figure 4-12 below, showed that;

1. Mean green (μ_G) was greater than both mean red (μ_R) and mean blue (μ_B) i.e. $\mu_G > \mu_B$ and $\mu_G > \mu_R$ for the samples,
2. The Excess Green (ExG) vegetation index normally used to identify vegetation based on RGB information especially from images that contain only visible light information (Ponti, 2013), for the tree crown samples had values greater than 0.18. It is computed as;

   $$ExG = 2G - R - B$$

   Where;

   $$R = \frac{R_C}{R_C+G_C+B_C}, \quad G = \frac{G_C}{R_C+G_C+B_C}, \quad B = \frac{B_C}{R_C+G_C+B_C},$$

   R_C = mean Red value for the segment,

   G_C = mean Green value for the segment and

   B_C = mean Blue value for the segment.

3. The tree crown to base ratio based on standard deviation in X, Y and Z values for each segment as illustrated in figure 4-13, for the samples had values greater than 0.17. It is computed as;

$$Crown_{base-height} = \frac{\sigma_Z}{\sqrt{(\sigma_X^2 + \sigma_Y^2)}}$$

where σ_X, σ_Y and σ_Z refered to standard deviation values in X,Y and Z for each segment.

4. Crown size was considered in form of segment size which had to be greater than 60 to prevent capture of small ground objects satisfying the preceding three stages.

These characteristics helped define the criteria for extraction of tree crown from the AOP point cloud.

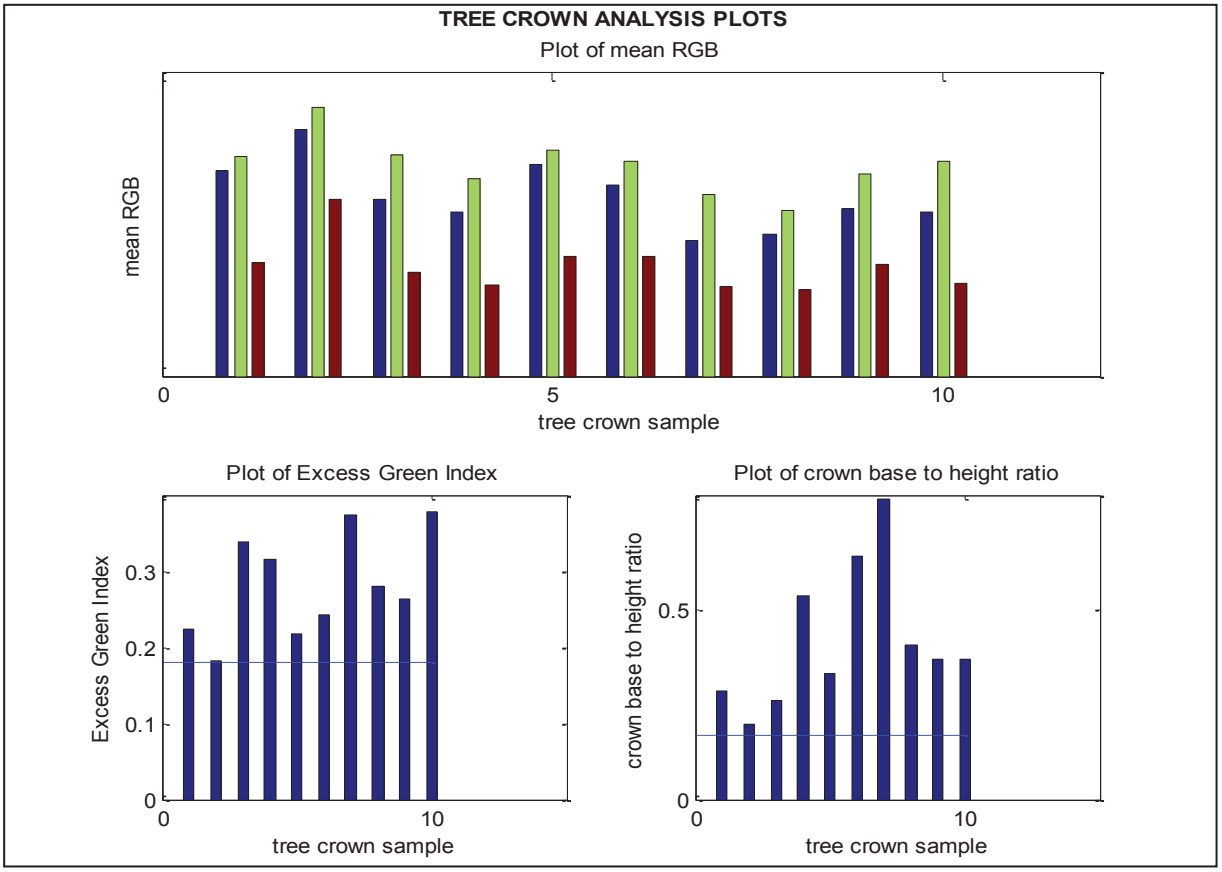

Figure 4-12. Sample tree crown features

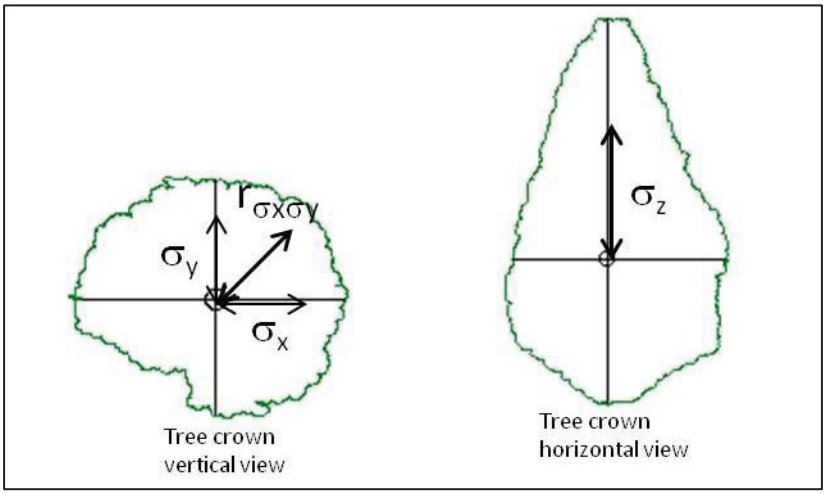

Figure 4-13. Tree crown form

4.5. Entities and features for entity extraction

4.5.1. Entities

The entities identified for target object extractions were plane segments and connected component cluster segments. This was because the target objects of this research entailed both planar objects and non planar objects. Walls, roofs and collapsed planes were all considered planar objects while tree crown was considered non planar objects, and rubble was considered to have a mixture of planar and non-planar objects. Given the planar nature of walls and roofs versus the clustered appearance of rubble and urban tree crowns, planar segments were preferred upon for wall and roof extraction while connected component clusters were preferred for rubble and tree crown identification.
Plane segments were created via plane segmentation and the clusters obtained by connected component.

4.5.1.1. Planar segments

The planar segments from the LiDAR point cloud were considered for roof segments while those from oblique point cloud were considered for wall segments. The plane surface nature of these target objects (roofs and walls) was the main consideration here. Given the vertical view captured by the LiDAR point cloud and its lower noise levels, it was considered the main input for detection of roof features. However given the absence of horizontal façade view from the LiDAR data, and the presence of the same in the oblique point cloud, the latter were considered as the main inputs for the wall object identification.

4.5.1.2. Connected component clusters (Non planar segments).

The clusters from LiDAR and AOP data were considered for rubble and vegetation identification respectively. The rubble clusters had high reflectance due to high sand content present from collapsed walls and roofs while the dominant green colouration of the urban tree crowns and their non planar shape that made them identifiable from their respective target input data. The green content attributed to the chlorophyll content in plants combined with the fact that the data was captured during the green foliage period of the trees.

4.5.2. Features for entity extraction

The features that were considered useful for identification of target objects were x,y,z component of the normal vector, inclination angle, segment size, mean X,Y,Z coordinates, mean reflectance, mean RGB values, the standard deviation in x, y, z coordinates of extracted entities. More specifically;

- The z components of the normal vector (computed for planar objects only) was found useful for differentiating walls from roofs i.e. wall had values < 0.3 while roofs had values > 0.7.
- The x and y components of the normal vector were found useful in identifying parallel walls or roofs, which tended to have similar or greatly close values. These were seen useful in computing the horizontal orientation of walls and roofs in form of their bearing direction.
- The inclination angle was found useful equally to separate walls from roofs (walls were inclined closer to the vertical while roofs tended to be further away), and it was equally used to differentiate tilted walls from the non tilted walls, and in identifying pairs of gable roofs.
- Segment size was a great consideration in identifying fragmented and collapsed planes.
- Mean X, Y and Z coordinates taken as mean segment position, i.e. defining the relative position.
- Mean reflectance was used to identify areas of rubble presence in conjunction with segment size, these areas had high mean reflectance and presence of relatively small segments around them.
- Colour content was used in identifying tree crowns, they had higher mean green than mean red and mean blue values, and in addition tree crown height to base ratio was equally used to identify tree crowns.

4.6. Definable Damage types.

The output in the final classification was to be based on damage classes as defined in the damage catalogue (Schweier & Markus, 2006). Given that input data for this research was limited to post earthquake data, there was need to determine identifiable damage types based on this data.
The requirements to facilitate determination of each damage type were reviewed against available data and the final status determined. The results were as presented in table 4-3 below.

Damage Group	Type	Requirements	Status given available data
Inclined layers	Inclined plane	wall planes, Roof planes	Determinable
	Multi-Layer collapse	Pre-collapse form, Wall planes, Roof planes.	Not determinable
	Outspread Multi-Layer collapse	Collapsed planes, Positional state, Geometrical state.	Determinable
Pancake collapse	Pancake collapse one storey	Roof Planes, Wall planes, Pre-collapse form.	Not determinable
	Pancake collapse several /all storeys	Roof planes, Wall planes, Pre-collapse form.	Not determinable
Debris heaps	Heap of debris on uncollapsed stories	Debris, Wall planes, Roof Planes.	Determinable
	Heap of debris with vertical elements	Debris, Wall planes	Determinable
	Heap of Debris	Debris	Determinable
	Heap of Debris with plates	Debris, Collapsed planes	Determinable
Overturn collapse	Overturn collapse separated	Wall planes, Roof Planes, Pre-collapse form	Not determinable
	Inclination	Wall planes, Roof planes.	Determinable
	Overturn collapse	Wall planes, Roof planes, Pre-collapse form.	Not determinable.
Overhanging elements	Overhanging elements	Roof planes, Wall planes, Pre-collapse form.	Not determinable

Table 4-3. Definable and non-definable damage types

The multiple layer collapse required knowledge on pre earthquake roof and wall structure form status. Pancake collapse required knowledge on the pre earthquake building height. Overturn collapse required

knowledge on the pre earthquake building foot print and construction plan and form. Overhanging elements required knowledge on pre earthquake building form. Given that this research had only post earthquake data in form of LiDAR and Aerial Oblique photography derived point cloud, the damage types definable based on post earthquake data were the ones to be considered. This meant that the damage types deemed to require pre-earthquake data were taken as non determinable damage types within the limits of this study. Illustrated and highlighted in red on figure 4-14 below are the graphical representations of the damage types identified as determinable.

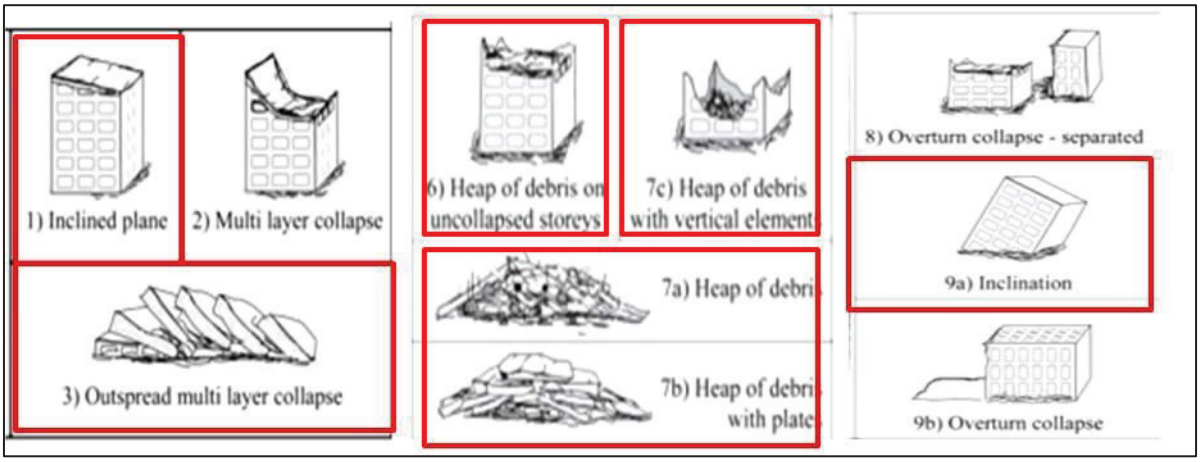

Figure 4-14. Definable damage types based on the damage catalogue(red boxes) (Schweier & Markus, 2006).

4.7. Analysis summary

From the analysis several key observations are noted;
First it becomes clear that planar segments facilitate the ease of identifying building parts as walls and roofs based on point cloud. Further, the non planar areas, especially rubble are easily covered in the point cloud clusters form. It is equally seen that given the form of any point cloud segment representing any building part can be analysed for damage within. This is exemplified by checking for presence or absence of tilt on the planar segments. Hence the relevance of point cloud, as it helps in capturing the true form of a building and objects within its neighbourhood..
Secondly, given the nature of input as post earthquake data only then its seen in section 4.6 which damage types are definable. Hence by linking the practical form of the true status of each building, the true picture of the overall damage status of each building is defined.
Third, it was found that noise levels were higher in the oblique point cloud compared to the LiDAR point cloud. This was a useful observation as it influenced the setting of plane segmentation and connected component process parameters. The plane segmentation for LiDAR point cloud had limits of points off the plane being set more restrictive compared to that of the Oblique point cloud.

5. METHODOLOGY

5.1. Introduction

The proposed approach involved direct use of object properties, based on 3D capture ability of point cloud data, a feat preferred compared to model based classification as the classification is guided truly by existent object characteristics within the study site. The input point cloud data contains coordinate information, is post earthquake data and has additional reflectance and colour information for the LiDAR pcl and AOP pcl, the damage types definable will be limited to these capabilities. Further, given the intent to assess damage based on the damage catalogue classes, the approach involved assessment of individual identified target objects to define the damage status of the building structure under consideration.

To perform the classification, first the characteristics of the desired target objects are identified and defined, with application of constraints based on the same characteristics. The applied constraints help in better understanding of the definition of extracted objects based on input point cloud data.

The input datasets were used preferentially based on their identified useful characteristics. The LiDAR point cloud given its vertical overview, better positional information and reflectance information was used for extraction of the roofs and rubble target objects and definition of planar building units. It was not used for walls and vegetation (urban tree) identification at it lacked the horizontal façade view and colour information The Oblique point cloud, given its horizontal facade view capability of containing building façade information and colour information within it was preferred for extraction of walls and urban trees.

For this method, given the normal approach to construction of buildings from foundations, through walls to roofs the same criteria was applied in extraction of target objects. Walls come first then roofs, and rubble and vegetation were extracted separately. The method involved five phases; first was pre-classification data processing, second was extraction of target objects, third was defining building unit, fourth was the practical definition of damage classes, fifth was the damage assessment cum classification and finally the evaluation process. The whole process is summarized in figure 5-2 below.

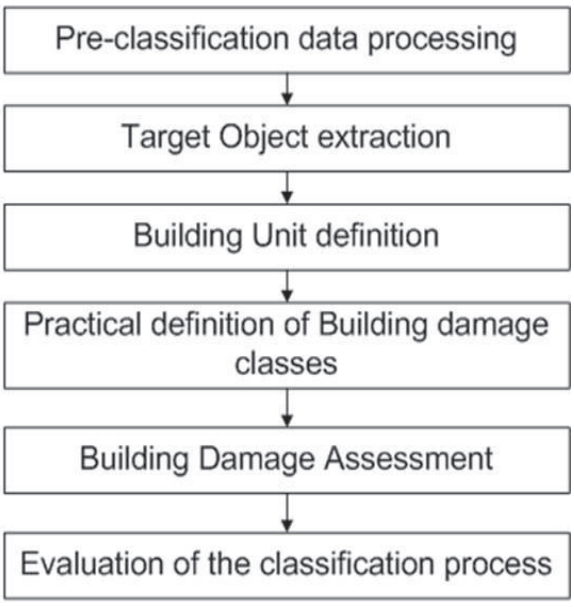

Figure 5-1. classification work flow in general

The approach directly employs extracted and defined characteristics to group segments into target objects of interest. This approach involving use of point cloud data has greater advantage of revealing desired object form in 3D compared to satellite imagery.

5.2. Pre-classification data processing

Point cloud in its raw form contains both useful and non useful information depending on the project at hand. This research focussed on buildings and related objects within their environment. Input point cloud data had to be structured into desired forms, from which target objects would be extracted. The process involved segmentation and clustering of the point cloud datasets, extracting plane and cluster segment features, and computation of extracted segment features as illustrated in figure 5-2. Despite the process being the same for both datasets, different settings were applied for each dataset due to the varying densities and noise levels for the two input point cloud datasets.

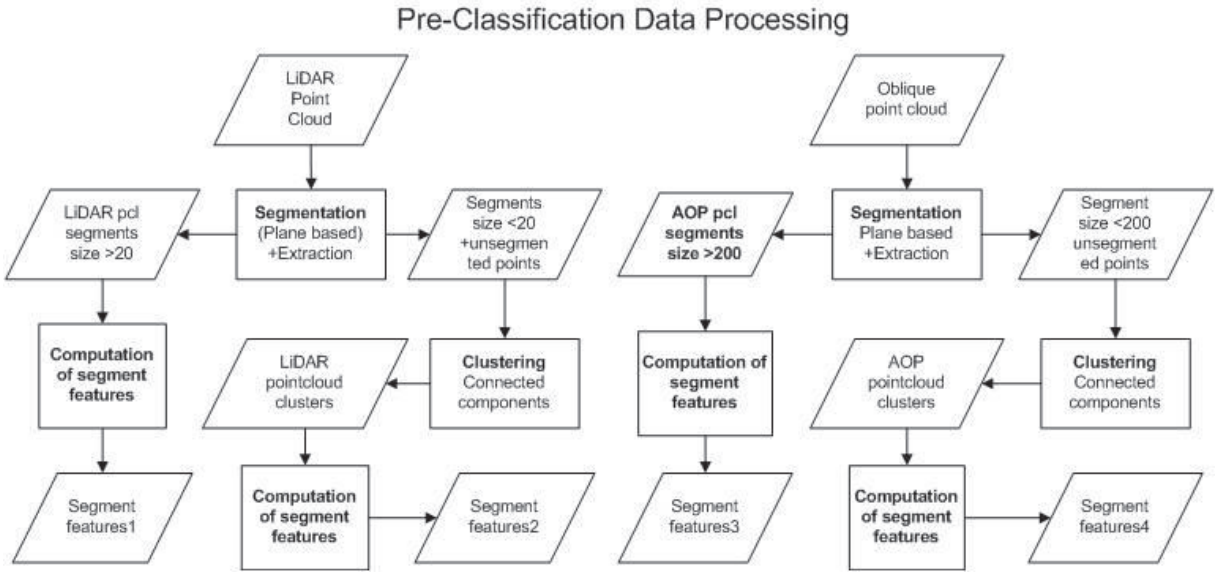

Figure 5-2. Pre-classification data processing

5.2.1. Segmentation

Plane based segmentation was used to create desired plane entities. It was informed by the fact that walls and roofs are always planar in nature. The surface growing method was used, with the data structured to k-D tree (Samet, 1990). However the higher noise levels in the Oblique point cloud meant that settings for segmentation parameters were more moderate compared to those of the LiDAR point cloud. Maximum distance to surface was set at 0.1 and 0.3 for LiDAR and Oblique point cloud respectively. However, informed by the decision that roofs and walls always have relatively large sizes, the extraction of segments was limited to segment size 20 for LiDAR point cloud and 200 for the Oblique point cloud, differences based on the second fact that the Oblique point cloud appeared to have higher density than the LiDAR point cloud. The aim was to separate plane entities for roof and wall extraction from those targeted for rubble and tree crown objects. The remaining point cloud was then forwarded on for clustering.

5.2.2. Clustering

Clustering in this case involved use of the connected components functionality of PCM software to form clusters of the remaining point cloud after segmentation planes had been extracted. Clustering was used to capture rubble and tree crown forms, that have non planar shapes not suitably captured by plane based

segmentation. The settings were different given the higher density in the Oblique than the LiDAR point cloud. In a scenario similar to zooming into the structure, the connected component maximum distance to point was set to 1.0 and 0.5 for LiDAR and Oblique point cloud respectively in order to ensure the smaller fragments and separations are captured. The higher density of Oblique compared to the LiDAR point cloud influenced this decision. The result was a collection of point cloud clusters suitable for input to extract target objects of interest, specifically the rubble and tree crowns respectively.
The products of the processes segmentation and clustering are illustrated in figure 5-3 below.

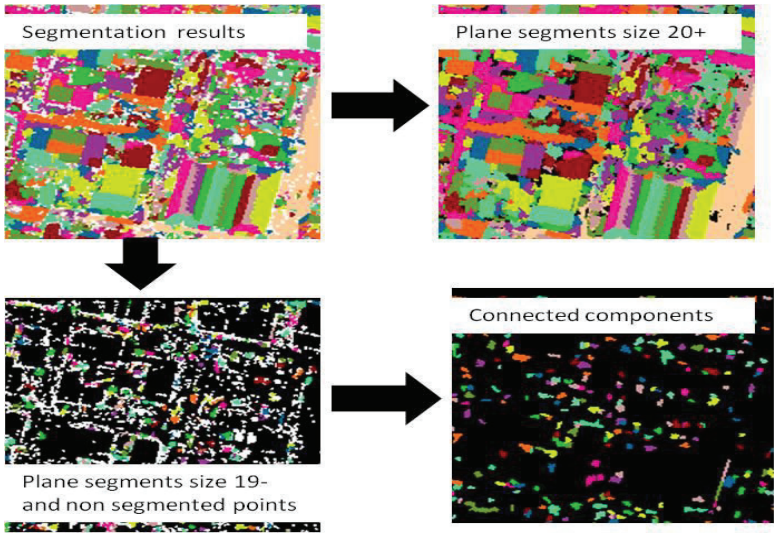

Figure 5-3. LiDAR point cloud segmentation and clustering

5.2.3. Computation of segment features

Several segment features were computed to facilitate the basic automation of the classification algorithm using a Matlab code, several segment features were computed depending on the input data source. Common to both datasets were;

- Mean of X, Y and Z, were the mean values for Easting, northing and Elevation coordinates of any point cloud segment or cluster.
- Minimum and maximum Z, minimum and maximum elevation coordinates of any segment.
- Standard deviation in X, Y and Z coordinate values.
- Segment size, total number of points in a segment.

Additionally for each segment based on the input data source;

- Mean reflectance was computed for the LiDAR based segments,
- Mean Red, Green and Blue was computed for the Oblique based segments.

Further, for the plane segments a mathematical plane fit process was carried out. This involved using a plane fitting equation in form of a Matlab code to compute the components of the normal unit vector defining each fit plane, and the perpendicular distance from the origin. The resultant x, y and z components of the unit vector provided input for computation of features as the inclination angles and horizontal orientation. This step was useful in providing the mathematical base that defined the extracted plane segments. Its usefulness was depicted in;

- Use of x and y components to define horizontal orientation (identify parallel objects).
- Use of x, y and z components to compute inclination angle, which combined with horizontal orientation helped identify gable roofs.

5.3. Extraction of target objects.

The main target objects of interest were the walls, roofs, rubble and urban trees (vegetation). Based on their natural status, the characteristics of the objects of interest were defined and used for extraction of the objects of interest. For the walls being planar in nature, their defining characteristics came from the results of plane fitting residual analysis and related components. Extraction followed a similar bottom up approach first walls, then roofs as in the normal building structural construction process. Further, following the content and form of the respective segments; Walls and roofs were extracted from Oblique and LiDAR plane segments respectively, while vegetation was extracted from Oblique connected component cluster segments while rubble was extracted from both LiDAR connected component cluster segments. The process is illustrated in figure 5-4 below.

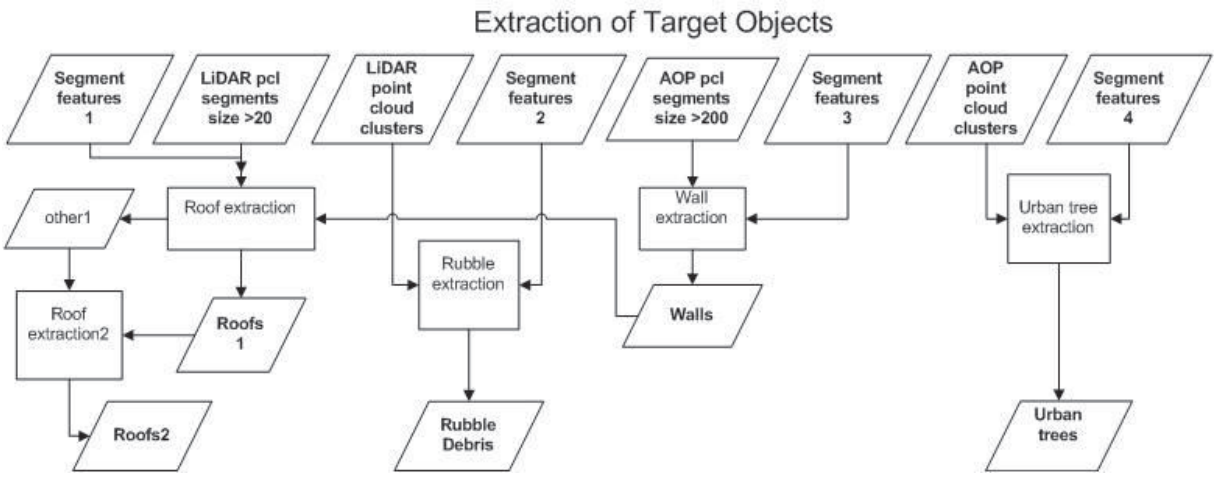

Figure 5-4. Extraction of target objects.

5.3.1. Walls

Based on their natural state of being in vertical or near vertical positions their characteristics were defined. These were taken as;

- Large segment sizes taken to be greater than 80 points.
- Having z component of normal vector not greater than (<0.3),
- Had smaller inclination angles (<20°) correlated with the smaller z components of the unit vector.

5.3.2. Roofs

Based on their status in nature of being above walls and inclined further from the vertical to the limit of having flat roofs, their characteristics were defined. These were taken as;

- Having larger z component of the normal unit vector, greater than 0.7.
- Had larger inclination angles greater 30°but less than or equal to 90°,
- Their minimum height (min Z) had to be at least 2m above the minimum height of surrounding walls i.e. $(Z_{\min\ roof} > Z_{\min wall} + 2m)$ or $(Z_{\min\ roof} - Z_{\min\ wall} \geq 2m)$,
- Their minimum height had to be equal to or higher than the height of the neighbour roofs (For higher roofs that had no walls captured around them)
- Had their minimum segment sizes greater than 30.

5.3.3. Rubble

These are usually taken as all manner of broken and collapsed material from buildings or parts of it collapsing. Given that having an overall single defining signature for rubble was not possible,

consideration was given to rubble elements from collapsed concrete structures. This was so due to their defining signature of spectrally having high mean reflectance values and broken pieces thus relatively small. Segment sizes and mean reflectance were the key features in identifying rubble piles. Considering this, the rubble definition for this research was the resultant cluster segments obtained after;

- LiDAR plane segments of size less than 20 and average reflectance greater than 115 that were,
- Clustered using connected components and those with mean reflectance above 115.
- Planes, those that were not taken as roofs or walls but lay within the neighbourhood of the rubble cluster identified using the first two characteristics, and having segment sizes greater than 20 but not exceeding 60. This was taken to incorporate broken building parts that lay around collapsed sand incorporated building parts.

5.3.4. General extraction procedure

Walls were extracted based on the characteristics enumerated in 5.3.1. Plane segments from the Oblique point cloud were analysed for those that satisfied the properties;

.

Roofs were then extracted based on the characteristics enumerated in 5.3.2. Plane segments from the LiDAR point cloud were analysed for those that satisfied the properties.
Roofs were then identified and classified in two sets.

The First set of roofs was extracted based on their minimum height above minimum height surrounding walls. They had to be at least 2m above minimum height of surrounding walls. Given the point cloud segments had a normal distribution then their standard deviation showed their spread typically covering about 70% of the points as shown in the Gaussian plot (section 4.3). This was used to define the search radius between walls and adjacent roofs. Combining the standard distance defined by the horizontal (planar) standard deviation of any particular roof and surrounding walls, a search radius was defined. This was a modification of the standard distance defined for spatial analysis as the total length obtained by the square root of the sum of squared standard deviation in X and Y directions for features or points around their statistical mean. Given the segments were composed of points, this helped in linking roofs to adjacent walls using their centres (point defined by mean X and mean Y of each segment) as illustrated in figure 5-5 below.

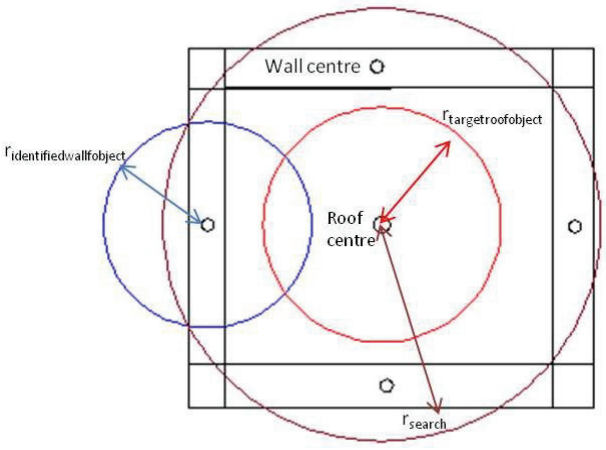

Figure 5-5. Roof identification based on existing walls

The search radius, radius of identified wall object and target roof object are as defined below.

$$r_{search} = r_{target\ roof\ object} + r_{identified\ wall\ object}$$

where

$$r_{target\ roof\ object} = \sqrt{(\sigma^2_{x\ roof\ target} + \sigma^2_{y\ roof\ target})},$$

$$r_{identified\ wall\ object} = \sqrt{(\sigma^2_{x\ wall} + \sigma^2_{y\ wall})}\ .$$

The second set of roofs was those high above in places with no wall around them. They were defined based on segment size, inclination angle and height relative to height of first set of identified roofs. Specifically they had;

- segment sizes greater than 30 ,
- inclination angles ranging from 30 to 90 ,
- their centres displacement from centres of one or more of the first set of classified roofs within 1.5 times the search radius defined by;

  $$r_{search} = \sqrt{({\sigma_{xroof1}}^2 + {\sigma_{yroof1}}^2)} + \sqrt{({\sigma_{xrooftarget}}^2 + {\sigma_{yrooftarget}}^2)}$$

  Where;

  $\sigma_{x\ roof1}$, $\sigma_{y\ roof1}$ and $\sigma_{xrooftarget}$, $\sigma_{yrooftarget}$ refers to standard deviation of X and Y of first identified roofs and second target roof objects respectively.
- Their minimum heights greater than or equal to the minimum height of first set of identified roofs i.e. $h_{roof2} \geq h_{roof1}$ or $h_{target\ roof\ object} \geq h_{identified\ roof\ object}$.

The relationship between roofs and walls is as illustrated in figure 5-6 below.

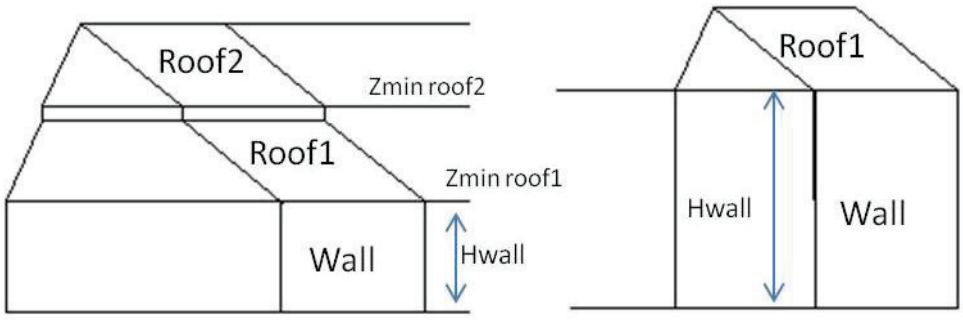

Figure 5-6. Roof and wall positional relation

5.4. Definition of the Building Unit

The building unit used was defined using the roof edges polygon and the rubble cluster set.

The first consideration using roof edges polygon was informed from the fact that the main output of most geospatial research works are presented in form of maps and plans, and in mapping science, building features as presented from the external vertical view appear in form of polygon shapes similar to the corresponding building roofs. Further, in many disaster response plans for earthquake affected areas as experienced during the Haiti earthquake key ground routes are usually destroyed limiting incoming assistance to be imported using airborne means. This means that the final damage assessment map, if it follows the roof shapes is easy to interpret and use by both local and foreign disaster response personnel familiar or not familiar with the local area. There the approach here involved projection of the roof plane on to the ground based on the X and Y coordinates of the edge points defining the polygon edge of any point cloud roof segment. The status of rubble, wall and roof segments within and on the edges of the

neighbourhood of this roof polygon would be analysed to give the final damage status. However, considering wall segments may have tilt and that their source data was the Oblique point cloud the roof polygons were always extended outward by 1.25m to capture surrounding walls and rubble. The extension involved use of matlab code extendPoly (Krispijn, 2009). The representative point for each wall, roof or rubble cluster was defined by the mean X and Y coordinate values.

The second consideration of building units were rubble clusters. This was especially so in cases of collapsed roofs thus rubble clusters form on top of storey buildings with two or more floors. The main link was the search radius defined as the combined standard distance of the rubble cluster and surrounding walls. The process of defining building units is illustrated in figure 5-7 below.

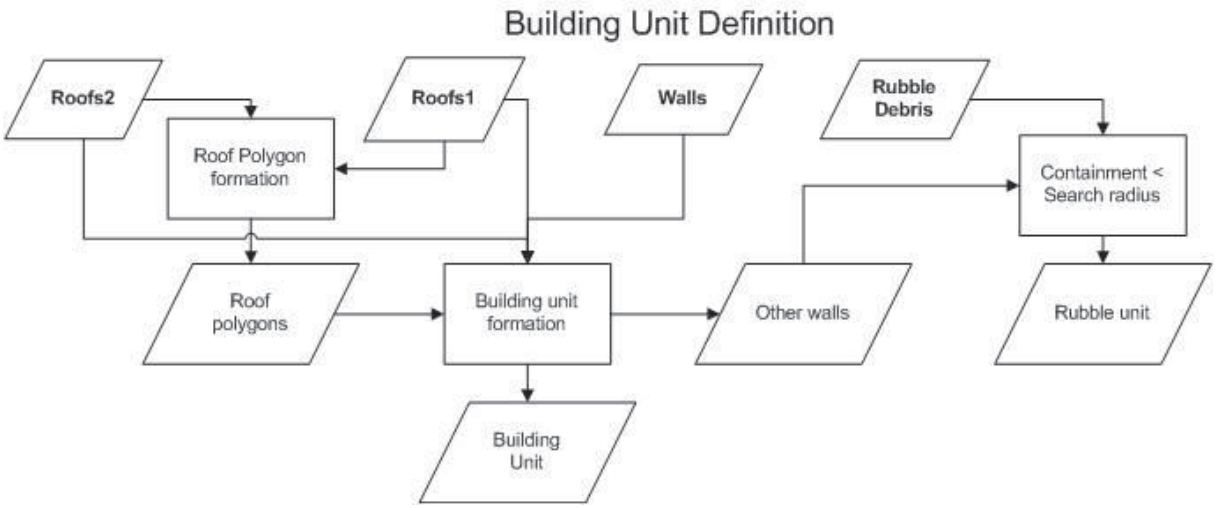

Figure 5-7. Defining building units

5.5. Damage Assessment

Damage assessment was implemented in a procedural, rule based classification process. The first step was checking presence or absence of tilt on roof and wall segments. This was followed by grouping of all walls, roofs and rubble within and along the edges of the identified building unit into one set. The set contents were then analysed based on the practical definition of damage types to give the final damage status of the building unit.

5.5.1. Determination of tilt.

Tilt was considered the leaning of a wall or roof structure off its assumed normal situation. The normal situation for walls was taken to be vertical or within 5 degrees angular deviation from the vertical. For roofs, the normal was taken as being completely horizontal for flat roofs while for gable roofs it was having the upper and lower edges being completely horizontal.

For walls, assumed to be vertical in nature, inclination angle from the vertical was used as a measure of tilt. Wall tilt was computed using formula for inclination angle (section 4.4.1).

Given the high noise level in the Oblique point cloud averaging approximately 30cm from the oblique point cloud standard deviation values($\sigma_{Oblique\ pcl} = \pm 15cm$) and taking walls to have a minimum of 3m height then vertical walls were taken as those with inclination angle from the vertical being less than or equal to 5 degrees. This is based on $tan^{-1}(\frac{30}{300}) = 5.7106^{\circ}$. Further tilted walls were taken as those whose inclination angle was greater than 5 degrees but less than or equal to 30 degrees.

$(tilted\ i_{angle} < 5°\ while\ non\ tilted\ 5° < i_{angle} < 30°)$ Tilt in walls is illustrated in figure 5-8 below.

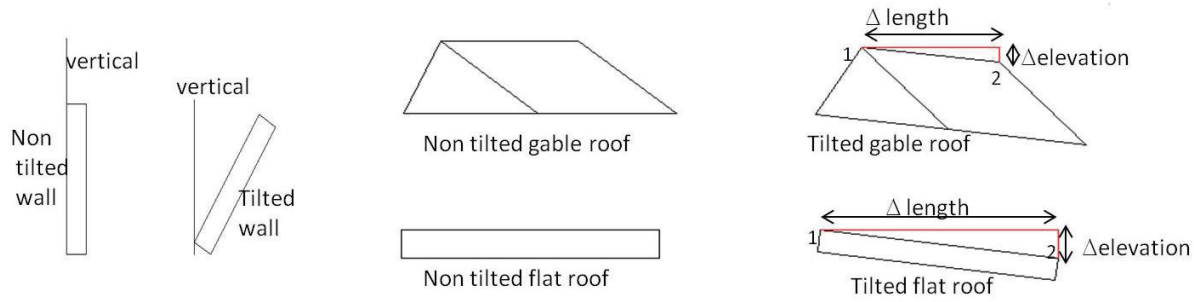

Figure 5-8. Tilt in walls and roofs

For the gable roofs, the slope orientation was used to determine presence or absence of tilt. Roof edge coordinates were extracted and the slope between successive points computed. Roof edge coordinates were extracted by constructing planar convex hulls of roof segments and then identifying the X,Y and Z coordinate values for these points. This was informed by the fact that for flat roofs all points would have slope values equal to zero or very close to this. For gable roofs, the upper and lower edges would also have values closer to zero. Tilt in roofs is as illustrated in figure 5-6 above. Thus taking a minimum of 5m length for roofs and getting the average noise level of the LiDAR point cloud being at 4cm $(\sigma_{LiDAR\ pcl} = \pm 2cm)$ then the slope limit was set at 0.008, given $(\frac{\Delta Z}{\Delta_{Length}}) = \frac{0.04}{5.00} = 0.008$. Thus tilt was present in all roofs which had at least one edge with slope value greater than 0.008. Roof tilt was computed for two edge points with coordinates (X_1, Y_1, Z_1) and (X_2, Y_2, Z_2) using the formula;

$$slope\ orientation = \frac{\Delta_{elevation}}{\Delta_{length}},$$

Where $\Delta_{elevation} = \Delta z = Z_1 - Z_2$ and $\Delta_{length} = \sqrt{(X_1 - X_2)^2 + (Y_1 - Y_2)^2}$.

5.6. Definition of Damage Classes

The identified damage classes sourced from the damage catalogue needed to be redefined practically based on the available post earthquake point cloud data. This meant giving consideration to the positional geometry of the identified target objects (walls, roofs and rubble). This decision was informed by the fact that geometrical features were the main factors considered during the development of the damage catalogue. There key considerations here were the segment size, inclination angles, general roof slope orientation and additional bright spectral nature of broken building concrete wall or roof features. Damage types considered here were inclined plane, outspread multilayer collapse, heap of debris and inclination.

5.6.1. Inclined plane

Inclined plane was considered in situations where all wall segments within the building unit had lacked any tilt and the roof had some presence of tilt as illustrated in figure 5-9. Features used for wall tilt were inclination angle from the vertical while for roof tilt was detected based on slope orientation of the roof edges. Parallel walls were detected based on their horizontal orientation with respect to the north. This was determined based on the bearing direction of the walls, using the x and y components of the normal unit vector.

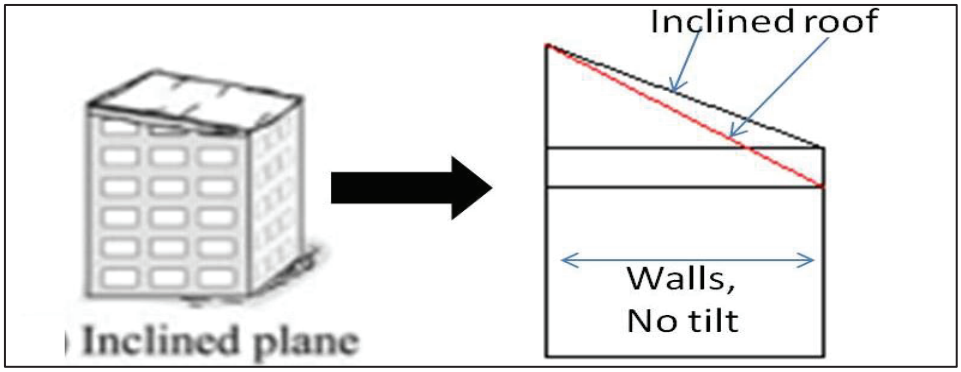

5.6.2. Outspread multilayer collapse

Outspread multilayer collapse was defined based on segment orientation, inclination angle, difference in mean heights and displacement of the planimetric position of segment centre points from each other. The plane segments not identified as either roofs or walls were considered target input for this. The criteria was to identify segments whose centre points lied within two times the standard deviation of the respective neighbour segment, the difference in mean height was less than 1m, their horizontal orientation orientations and inclination angles did not differ by a significant margin (<25°). However the seed segment must have rubble within its search radius. From this the we check for availability of small plane segments within its neighbourhood (centres of such plane segments must be within 2 times of the search radius) with mean height difference not exceeding 1m, and difference in inclination angle not exceeding 25 degrees. Outspread multilayer collapse is illustrated in figure 5-10 below.

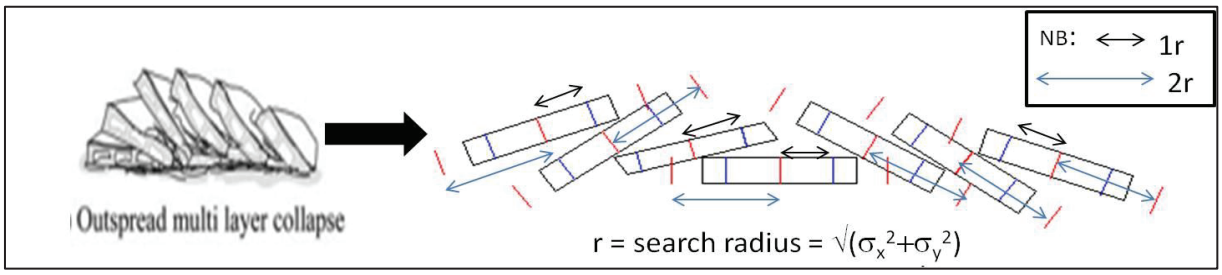

Figure 5-10. Outspread Multilayer Collapse

5.6.3. Heap of debris

Heap of debris was considered in areas where the initial heap of debris was identified (section 5.3.3), and further extended to plane segments of sizes between 20 and 100 that had not been classified as walls, roofs or used in the outspread multilayer collapse damage type. Those that were found to have their centres falling within the search radius ($r_{search} = \sqrt{(\sigma_x^2 + \sigma_y^2)}$) of the rubble cluster and unclassified plane segments in consideration. Further, their difference in mean height was not to exceed1m to be considered for the class heap of debris with plates. Figure 5-11 illustrates heap of debris damage type.

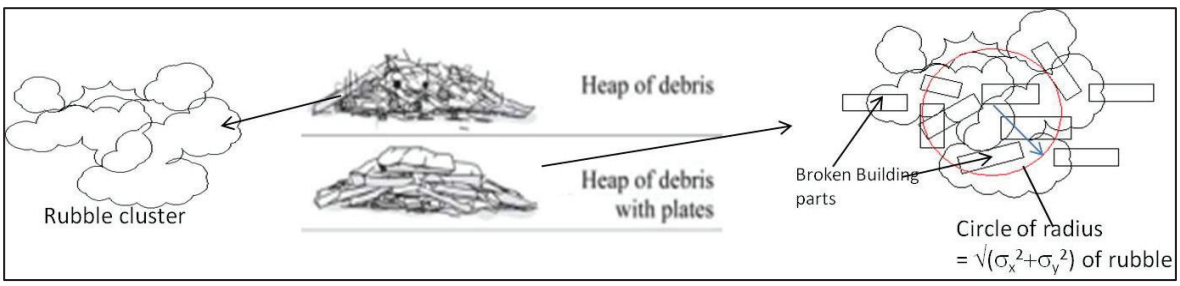

Figure 5-11. Damage classes Heap of Debris and Heap of Debris with Plates

5.6.4. Heap of debris on uncollapsed storeys

Heap of debris on uncollapsed storeys was identified by comparing the difference between the mean height of identified rubble and the minimum height of surrounding walls. The average height of walls from buildings with at least first floor was taken to be 5m on the lower side. Consideration was then given to heap of rubbles found having their mean height being 5m or more higher than the minimum height of walls within 1.5 times its search radius ($r_{search} = \sqrt{(\sigma_x^2 + \sigma_y^2)}$), as illustrated in figure 5-12.

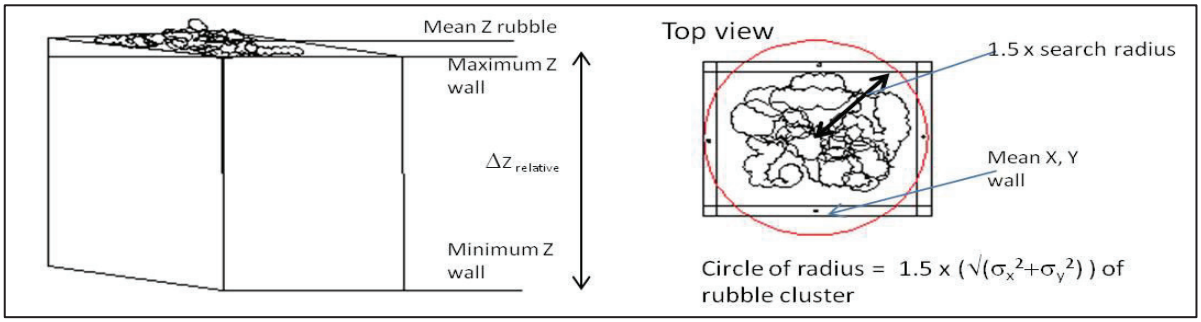

Figure 5-12. Heap of Debris on Uncollapsed Storeys

5.6.5. The inclination

This was considered in cases where presence of tilt was detected in both roof segments within and wall segments within or on the edge of building unit. Cases where tilt was present in one set of parallel walls and the roof segment were also considered to belong to this class. A set of parallel walls consisted of a group of walls with the same horizontal orientation.

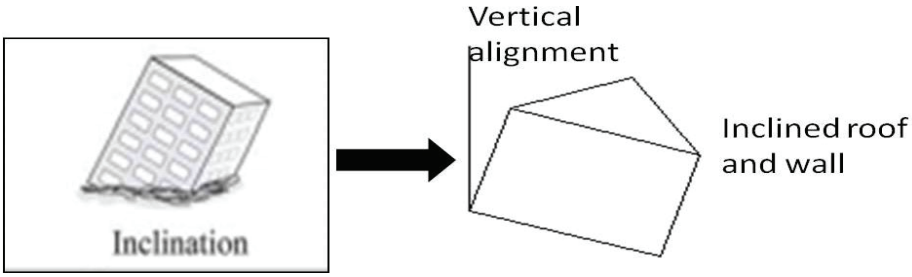

Figure 5-13. Inclination damage class

5.7. Overall Damage Classification

The overall damage classification strategy was based on the above defined damage classes. Each building unit was analysed for presence of characteristics satisfying the defined damage classes as above.
The classification was procedural, with characteristics of each damage class as defined in section 5.6 providing the rules for determining the damage status of each building unit.
The procedure entailed;

- Identifying walls within each building unit. These were then grouped based on parallelism using their horizontal orientation or bearing. Walls within each parallel group were then scrutinised for presence or absence of tilt. Grouping of walls based on parallelism helped identify pattern of tilt.

- The second step involved identifying roof segments within the building set. These were then grouped based on inclination angle and horizontal orientation to check for pairs of gable roofs. The final step was examining if roofs with similar inclination angles had or had no tilt present.
- The third step involved checking for rubble clusters, and if they had their mean height closer or further from the minimum height of surrounding walls. Further, for rubble clusters with additional broken plates around them were checked for the presence of the outspread multi layer damage class.
- The fourth step involved comparing relative mean height of identified rubble and the minimum height of surrounding walls. The difference in height was checked to see if it exceeded 5m. For values greater than five metres, consideration was given to the damage class heap of debris on uncollapsed storeys.

The result of the classification process was portrayed using colour information on the roof plane segment or rubble unit segment projected on to the zero elevation planes. That was then taken to be the damage status of the building unit under consideration. The results of the classification process were then taken for evaluation of the classification process.

6. RESULTS AND DISCUSSION

Results and discussion includes the results of target object extraction and damage classification, the evaluation of the classification results and the discussion of the results at different levels. The results for this research were the output of identified target objects of interest (walls, roofs, rubble, and tree crowns) and the output of the damage assessment. The first main part illustrates extracted sample gable roofed building, flat roofed building and tree crowns, with brief description of their characteristic features. The succeeding part shows site wide classification results, followed by statistical evaluation of the classification results and finally the discussion of the classification results.

Illustrated below in Figure 6-1 is part of the results of the extracted objects of interest. The objects are differentiated by colour and pattern for ease of identification. Roofs are blue lines, Walls are Red, Urban tree crowns are green and Rubble is in yellow. The scenario depicts what is repeated throughout the study site, where walls are generally located around the edges of roofs. Tree crowns are located in areas of limited space next to buildings. Rubble (bright broken concrete pieces) are located in areas around partly or fully collapsed building structures.

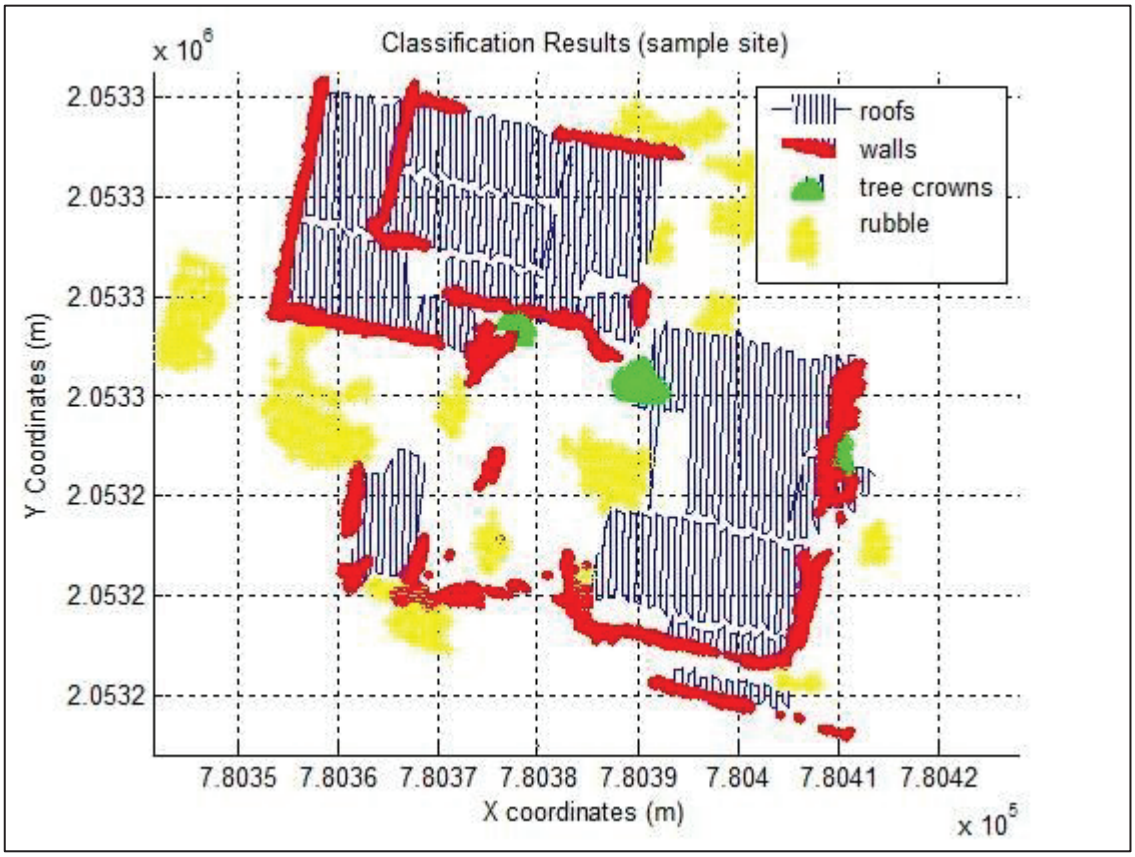

Figure 6-1. Sample site classification results

6.1. Sample entity and features results

The two main entities used to extract objects of interest were plane segments and cluster segments. They provided useful form for extraction of objects of interest. Further, several combination of features were used to obtain unique identifying combinations to facilitate extraction of objects of interest. Sample details

on these are presented as flat roofed building, gable roofed building, urban tree crown and rubble site, and accompanying description.

6.1.1. Flat roofed building

This consists of a building whose rooftop is generally parallel to the horizontal surface as illustrated in figure 6-2. The plane segments were the useful entities considered here. Features used are the components of the normal unit vector, minimum and maximum height, segment size, and inclination angle as presented in table 6-1.

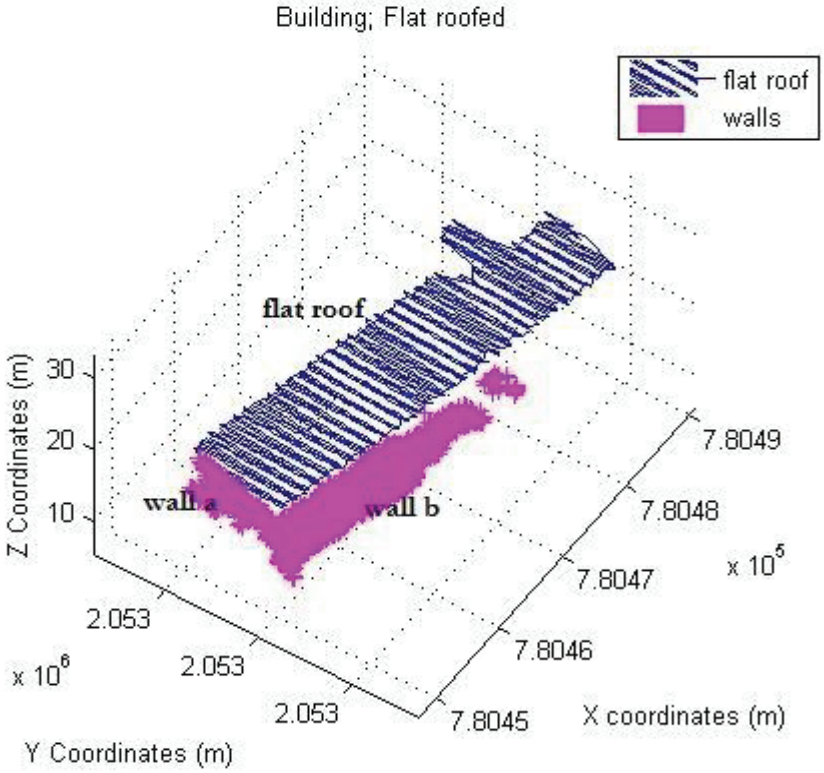

Figure 6-2. sample flat roofed building

FLAT	x_unit	y_unit	z_unit	minZ	maxZ	seg_size	i_angle	h_bearing
roof	0.00129	0.00695	-0.999975	21.86	22.48	2502	89.59497	0.183528
wall_a	0.95747	-0.209143	0.198773	14.15	24.35	391	11.42987	102.32775
wall_b	0.234955	0.970294	-0.057672	14.68	22.94	1416	3.088968	13.520667

Table 6-1. sample flat roofed building features

6.1.2. Gable roofed building

Gable roofed building usually consists of a pair of roofs inclined from the horizontal as illustrated in figure 6-3. Plane segments are the main input entities of consideration. Features found useful are the components of the normal unit vector, minimum and maximum height, segment size, inclination angle and horizontal orientation as presented in table 6-2.

GABLE	x_unit	y_unit	z_unit	minZ	maxZ	seg_size	i_angle	orientation
roof a	0.05698	0.251743	0.966115	15.93	17.95	214	75.042	12.753528
roof b	0.054858	0.254239	-0.965584	15.91	17.97	205	74.9302	12.187578
wall a	0.976046	-0.21586	0.027198	3.84	15.04	580	1.548448	102.47913
wall b	0.230302	0.972549	-0.0333	3.19	12.42	122	1.908293	13.322394
wall c	0.282032	0.947359	-0.151557	12.61	18.15	169	8.717174	16.578427
wall d	0.095933	0.99245	-0.076421	6.96	18.5	286	4.382849	5.521211
wall e	0.175672	0.984447	-0.001689	3.2	14.56	614	0.155693	10.146961

Table 6-2. sample gable roofed building features

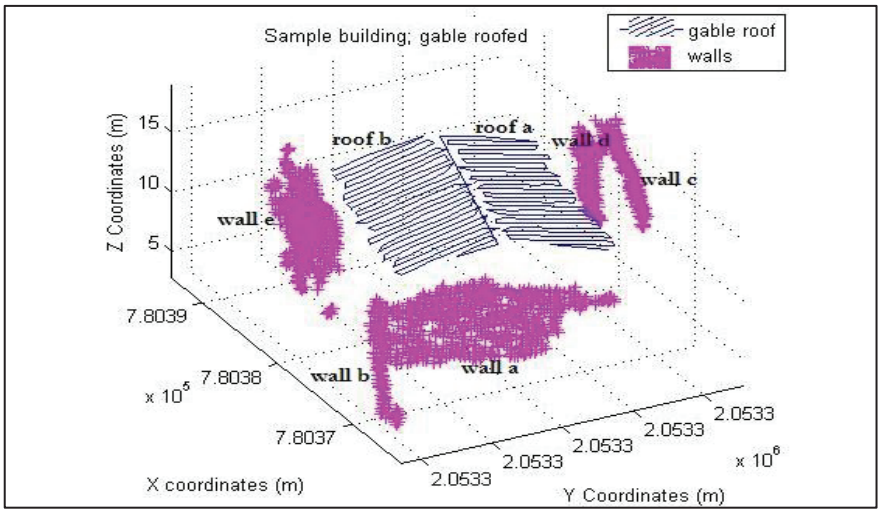

Figure 6-3. sample gable roofed building

6.1.3. Urban tree crown

Urban tree crown consist of non planar cluster of points dominated by the green colouration as illustrated in figure 6-4. The main features used in their detection are colour information (mean RGB), standard deviation in x, y and z, and segment size. Derived features based on these and found useful were the excess green index and the tree crown base to height ratio as presented in table 6-3.

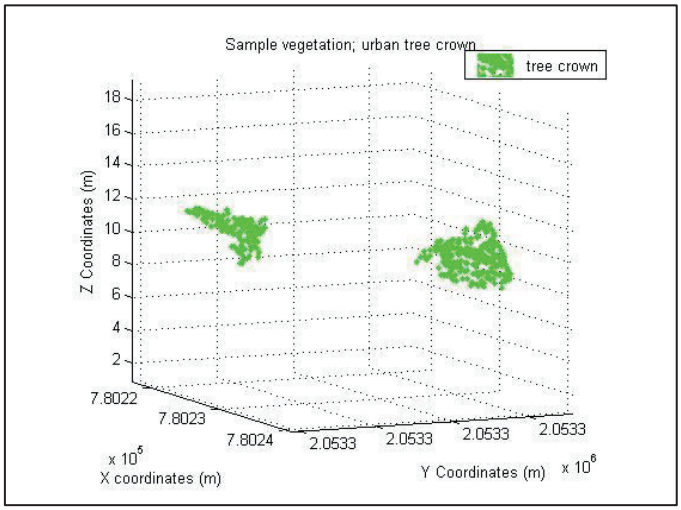

Figure 6-4. Sample Urban tree crowns

TREE CROWN	meanX	meanY	meanZ	minZ	maxZ	stdvX	stdvY
crown a	780227.5	2053271.749	11.266885	9.49	12.52	0.934292	1.123104
crown b	780230.1	2053285.991	9.152795	7.55	10.95	1.470866	1.082038
TREE CROWN	stdvZ	seg_size	mean_R	mean_G	mean_B	ExG	crown_b_h
crown a	0.70541	122	36.967213	51.663934	30.19672	0.309847	0.482856
crown b	0.754392	229	45.689956	62.847162	29.41921	0.374265	0.413141

Table 6-3. Sample urban tree crown features

6.2. Site wide classification results

This includes the results of site wide wall and roof classification, and the results of the damage assessment process in map form. This was aimed to visualize the picture of the final classification process.

6.2.1. Wall classification results

Wall objects extracted are presented in planar form on figure 6-5. The typical scenario is that of walls being vertically upright or close to this. The figure shows that consideration was on two classes of walls, tilted and non tilted walls. The non tilted walls being in blue while the tilted walls being in cyan colour. The key entity used here was the plane segment. From the figure it is relatively clear that tilted walls form a slight majority over non tilted walls, sort of indicating the effect of the lateral force of the earthquake.

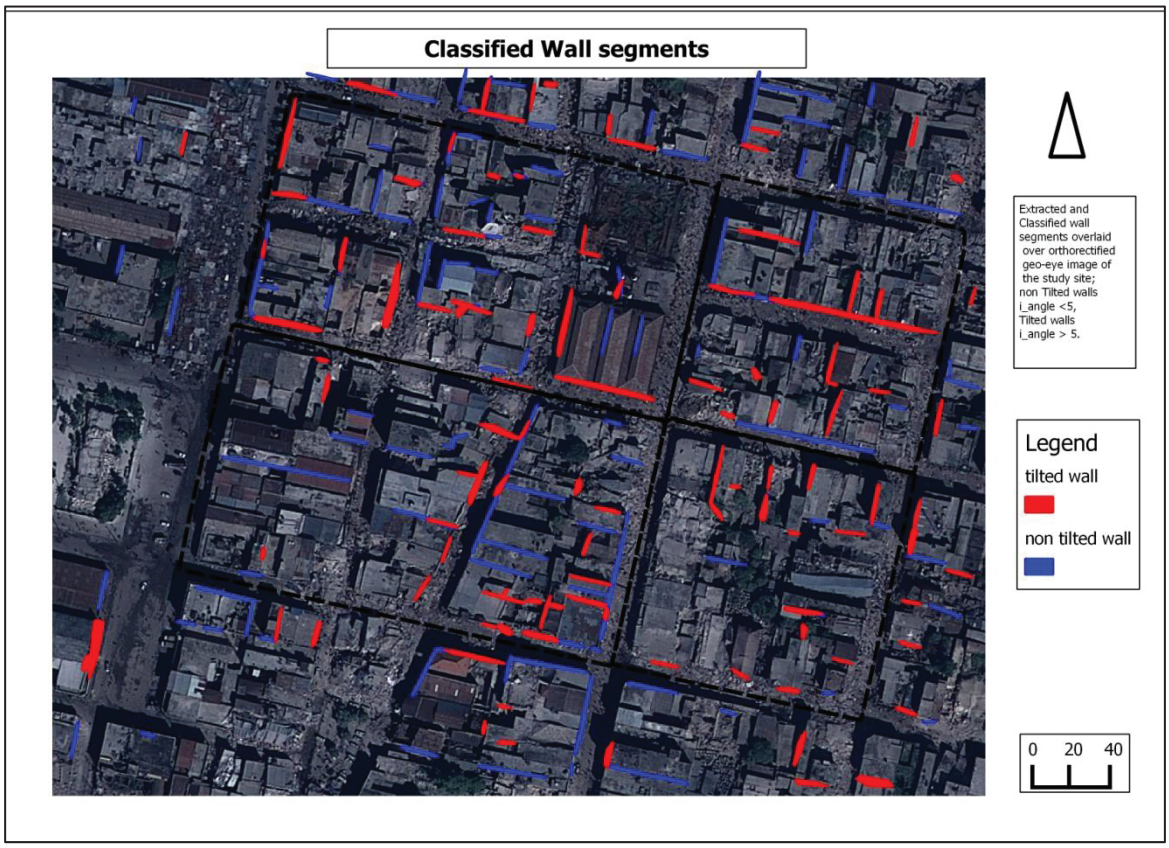

Figure 6-5. Classified wall segments

6.2.2. Roofs classification Results

Roof classification results are as presented in Figure 6-6 and 6-7. The typical scenario is that of roofs being above walls. The figure shows that consideration was given to two scenarios;

- Sets of gable /inclined roofs and flat roofs.
- Sets of tilted and non tilted roofs.

The gable roofs and flat roofs are depicted in blue and pale red colours respectively. The key entity used here was the plane segment. From the figure it paints a picture of the area being dominated by flat roofed buildings.

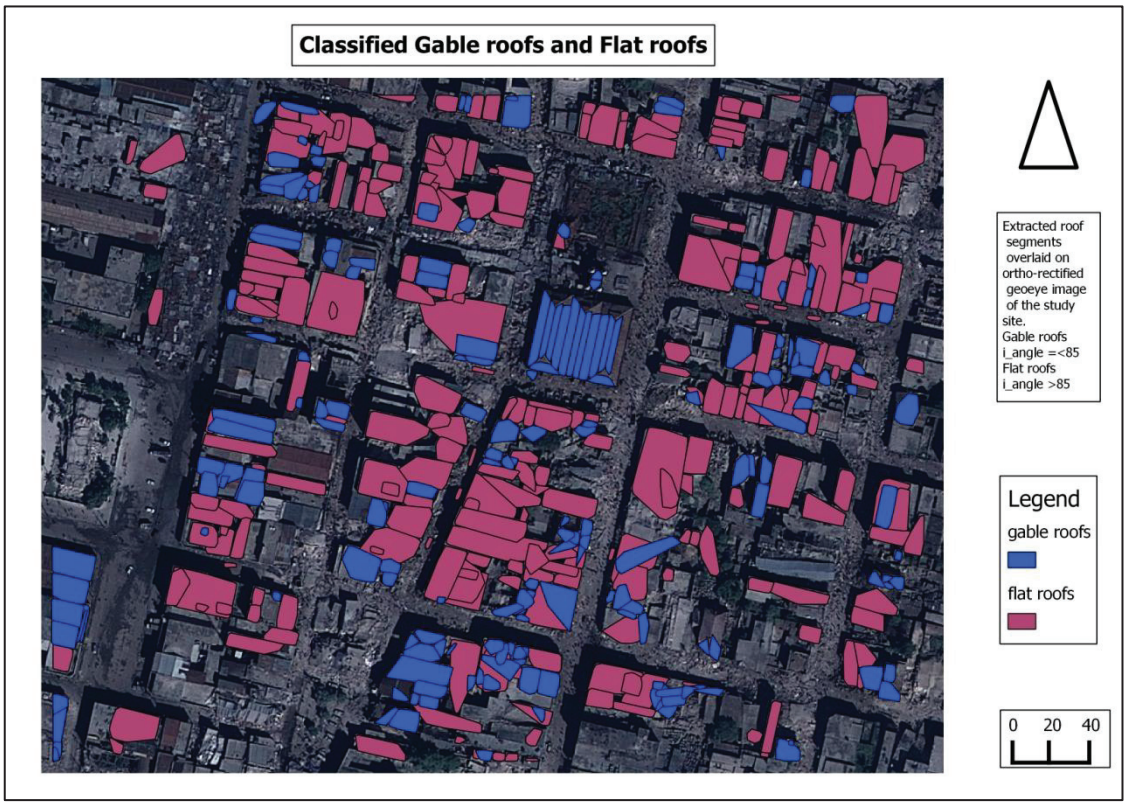

Figure 6-6. Gable and Flat roof classification

6.2.3. Damage Classification Results

Damage classification was carried out on the basis of the damage classes identified usable from the damage catalogue (Section 4.6). Damage classification in line with damage classes No tilt, Inclined and Inclination is as illustrated in figure 6-7. It can be seen that damage class no tilt forms a majority of the structures due to the fact that minor damages cannot be detected from laser data.

Heap of Debris taken as rubble was identified as illustrated in figure 6-8. The key consideration was segment size and reflectance value, given the high presence of sand component on collapsed building material. From the figure it is quite clear that not all heap of debris was identified given the definition of rubble applied in this research (sections 4.3.3 and 5.3.3).

Figure 6-7. No Tilt, Inclined and Inclination damage classes

Figure 6-8. Rubble / Debris sites

Roofs were further classified into tilted and non tilted roofs as illustrated in figure 6-9. Consideration was given to presence or absence of horizontal slope along the main edges of flat roofs, and the upper and lower edges of gable roofs. From the figure it is quite evident that a few roofs are actually tilted, however the situation may vary on the ground.

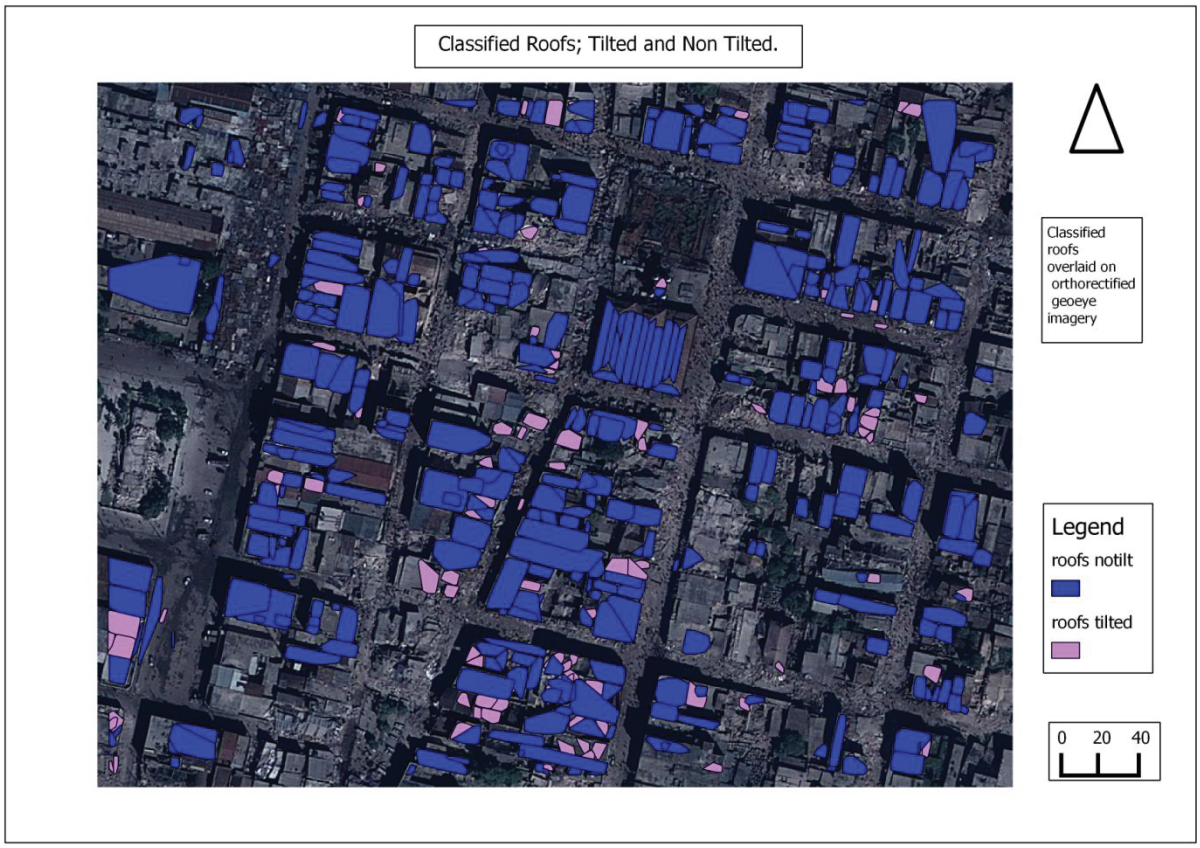

Figure 6-9. Roofs, Tilted and Non Tilted

6.3. Evaluation of classification results

Evaluation of the classification results involved determining the quality, completeness and correctness of the classification process. This entailed determining the number of target objects truly classified, those falsely classified and those existing on the site but not classified that was to enable determine the true positive (TP), false negative (FN) and false positive respectively (Rutzinger, Rottensteiner, & Pfeifer, 2009). The area was divided into four regions and the statistical evaluation carried out. The four regions are illustrated in the figure 6-10. The definitions of completeness /detection rate /producer's accuracy, correctness /user's accuracy and quality are as indicated below.

$$Completeness = \frac{TP}{TP + FN}$$

$$Correctness = \frac{TP}{TP + FP}$$

$$Quality = \frac{TP}{TP + FP + FN}$$

Figure 6-10. Evaluation zones

6.3.1.1. Rubble evaluation

Taking completeness, Correctness and Quality as defined above, the rubble results are as;

Rubble	TP	FN	FP	Completeness	Correctness	Quality
Zone 1	41	15	32	0.732143	0.561644	0.465909
Zone 2	40	9	18	0.816327	0.689655	0.597015
Zone 3	24	18	11	0.571429	0.685714	0.45283
Zone 4	29	19	25	0.604167	0.537037	0.39726
overall	134	61	86	0.687179	0.609091	0.476868

Table 6-4. Rubble Evaluation Results

From the results it becomes clear that the classification strategy adopted for rubble was not as good as expected. This may be attributed to the high number of small objects that equally had high reflectance values hence misclassified as rubble, and the presence of rubble in areas not related to collapsed concrete wall features.

6.3.1.2. Roof Evaluation

Roofs	TP	FN	FP	Completeness	Correctness	Quality
Zone 1	70	27	4	0.721649	0.945946	0.693069
Zone 2	51	11	6	0.822581	0.894737	0.75
Zone 3	17	11	0	0.607143	1	0.607143
Zone 4	81	24	1	0.771429	0.987805	0.764151
overall	219	73	11	0.75	0.952174	0.722772

Table 6-5. Roof Evaluation Results

For the roof classification the results were fairly successful. This was attributed to the large nature of roof planes that were easily detectable, with false positives occurring in areas that had high rubble accumulations and large vehicle bodies that were parked next to buildings. False negatives were attributed to areas that no wall was detected hence, the roof above was not classified.

6.3.1.3. Wall evaluation

For walls, it was taken that the outer walls, facing the main roads had to be at least visible hence evaluation was limited to these group of walls. This was because; the walls behind narrow alleys and in most building backyards were not captured or partly captured in the input data.

Wall	TP	FN	FP	Completeness	Correctness	Quality
Zone 1	39	12	3	0.764706	0.928571	0.722222
Zone 2	18	13	2	0.580645	0.9	0.545455
Zone 3	17	6	2	0.73913	0.894737	0.68
Zone 4	43	13	4	0.767857	0.914894	0.716667
overall	117	44	11	0.726708	0.914063	0.680233

Table 6-6. Wall evaluation results

The results for wall classification were fairly successful with false positives occurring on areas that had large linear features spanning across roof tops. The false negatives were attributed mostly to areas that had no or inadequate point cloud data coverage which created lack of or presence of small segments that did not meet the threshold of minimum wall segment size.

6.3.1.4. Urban tree crown evaluation

For tree crowns, since there few, the analysis was taken for the four zones combined.

Wall	TP	FN	FP	Completeness	Correctness	Quality
Zone all	25	5	7	0.833333	0.78125	0.675676

Table 6-7. Tree crown evaluation results

From the results it becomes clear that the tree crown identification and classification process was relatively successful. The high completeness and correctness values being an indicator of this successful classification.

6.4. Discussion on Classification Results

6.4.1. Discussion on damage classes

The damage classes identified were heaps of debris, inclination, inclined and no tilt. The process entailed analysing collection of wall and roof features falling within each building unit to gain the overall picture of the damage status. Based on figure 6-7, it is clear that the class no tilt has more units within it followed by inclination then lastly inclined. For the heap of debris or rubble as illustrated in figure 6-8 it was spread out wide throughout the site. This is an indication of quite a number of building parts having collapsed on broken off during the earthquake or as a result of follow up after shocks. However, given there was no ground truth sample data to verify the damage classification results, accuracy of this classification process is limited to accuracy of classification of the target objects.

6.4.2. Discussion on walls.

The walls were identified based on the criteria outlined in 5.3.1. All the sample walls were identified because of their being captured by the AOP point cloud. However, overlaying all walls identified onto the geoeye ortho image presented a realisation that not all walls were captured. This was attributed to two factors; the wall was not captured by the oblique point cloud or the wall segment size was small as it had been captured but not in its entirety. This equally revealed that segment size was a key feature in identification of wall segments. Setting a very low limit on segment size would capture small vertical segments that were not actual walls and equally raising the segment size limit would isolate walls captured but not in entirety during the formation of the AOP point cloud. Equally important was the realisation of the value of the x, y and z components of the normal unit vector. These were useful in computation of inclination angles, a key input in identifying tilted from non tilted walls. The relatively high values of completeness (0.727) and correctness (0.914) however showed success of the classification.

6.4.3. Discussion on Roofs

The roofs were identified based on the criteria outlined in 5.3.2. Not all sample roofs were identified. This was attributed to the weakness of the criteria where the main roofs were considered to at least have one wall under them. In areas where no wall was identified it consequently meant that roofs in that area would not be captured. However, features found useful in wall identification were the segment size, height information, inclination angle, horizontal and slope orientation. Segment size helped separate key input segment s from other unsuitable segments. Height information helped ensure identified roofs were above the minimum height of surrounding walls by 2m. This was in assuming that the lowest of roofs had their lowest point at least 2m above ground. Inclination angle was key in separating flat roofs from gable or inclined roofs. Flat roofs were taken as having inclination angles greater than 85°, while inclined roofs had their inclination angles ranging from 30 to <85°. Key to this was the components of the normal unit vector that were used to compute the inclination angles. Another key feature was the horizontal orientation or bearing of the roof segment. Horizontal orientation in combination with the inclination angle was helpful in identifying the pairs of gable roofs that had similar values for both horizontal orientation and inclination angle. Slope was also a key feature in identifying tilted from non tilted walls as illustrated in figure 5-6. Calculating the slope between points forming the outer edge of roofs deemed useful in identifying presence or absence of tilt on roof features. The main weakness was in cases where a previous gable roof had slipped into position making it lie flat hence identified as flat roof. Another weakness is the fact that segmentation planes may not actually resemble the true form of roofs as visualised on the Aerial Oblique Photographs, hence identified roof segments occupy the same representative position as on the image but may vary in segment form or shape and appearance.

6.4.4. Discussion on Rubble objects.

Rubble or heaps of debris were identified in this study using the criteria outlined in 5.3.3. The results proved less successful than expected. This was because of the rubble identification criteria that considered high reflectance and small segment size, that was common to many other building parts that were not within the rubble areas. However, there were other heaps of debris that were not from broken concrete parts that were not identified as they did not satisfy the criteria applied here. Key features used here were segment size and mean reflectance values. Segment size was key in identifying key small objects considered for rubble identification and the high reflectance values helped distinguish those that were rubble features. Further use by association was of segment size, given that broken plates around these identified rubble sites were equally part of the debris too. The process borrowed the idea of plane segmentation that identifies seed points and expands on them to identify plane objects.

6.4.5. Discussion on Urban tree crowns.

Urban tree crowns were identified based on the criteria outlined in section 4.4.4. The main features found useful here were the colour information, form and segment size. Colour was the key feature given the green nature of tree crown foliage within the study site. Mean green values and excess green index were computed and used to identify target candidate segments for tree crown identification. To further distinguish tree form, the crown nature was captured using the x, y and z standard deviation values of target tree crown segments as illustrated in figure 4-10. Tree crown height to base ratio computed using the x, y and z standard deviation values helped separate further tree crowns from target segments. Finally segment size was used to separate small objects that were not actually tree crowns. Tree crown were considered for this study on building damage, as a way of identifying possible locations of survivors and relief assistance sites. This is due to the common safety measure of advising people to avoid buildings especially in times around the occurrence of any earthquake until satisfied safe.

6.5. Discussion on Methodology

The approach methodology of using dataset characteristics to identify target objects of interest is found useful in successful object classification. However, the sequence of extraction of objects is a key weakness in the approach. This is exemplified by the case where if no wall is identified, it consequently means no roof will be identified even if existent. This is due to the consideration that the first set of roofs must occur above existing walls. The way to avoid or improve this is by ensuring the input dataset; in this case the AOP point cloud has no blind spots or areas with incomplete coverage.
The damage assessment part proved fairly successful as all identified roofs and wall features are given a specific class on whose criteria they satisfy. However, the main weakness may arise from different interpretations of the damage classes especially for the practical algorithm formed to implement the process. Further, in cases of misidentified target objects then the classification is equally vulnerable as its input is fully dependant on the identified target objects as rubble, walls and roofs.

7. CONCLUSION AND RECOMMENDATION

7.1. Findings on each research question

For this research there were several findings in line with the objectives and research questions as enumerated below.

- What is the relevance of point cloud data for building classification?
  - Given the ability of point cloud to depict geometrical form of any structure captured in the data then it helps in identifying the true status of each building part. The vertical view of LiDAR helps capture the roof features while the horizontal view of the Oblique point cloud helps capture the wall features. Further given the additional information contained in form of reflectance and colour helped in identification of rubble and vegetation respectively. Hence the relevance of point cloud data in helping capture and analyse the structure of target objects and buildings by extension.
- How will damage buildings be defined based on point cloud data?
  - Damaged buildings are defined based on the damage classes defined in the damage catalogue. However, it is the unique ability of point cloud to depict true form (planar or cluster) status thus capturing status of buildings, rubble and associated features. And on analysing these characteristic features, the final status of damage to the particular building is then defined.
- What is the level of noise in the input datasets?
  - The level of noise is as depicted by the plane fitting analysis in section 4.2 that shows higher noise levels in the oblique point cloud compared to the LiDAR point cloud. This is evidenced in the larger standard deviations of AOP datasets values >8cm compared to LiDAR datasets with values falling below 6cm.
- How does noise influence the extraction of entities from point cloud data?
  - Noise is considered in setting up parameters for the plane segmentation and connected components analysis process. This is so as higher noise levels means less stringent settings for the extraction of plane features. Further, the search radius of connected component entities is set up in an appreciable manner. Maximum distance to surface for LiDAR was set to 0.1m while that of the AOP dataset was set to 0.4m.
  - Further, given the observation of low noise levels in the LiDAR dataset, then the noise level influences the selection of the true surface. In this case the LiDAR fit surfaces were considered to be the true representative surfaces except for areas that require facade view as on building walls.
- What features of extracted entities are relevant for damaged buildings?
  - Given the need to define damage based on the damage catalogue classes then features that help define the geometry and form of buildings and rubble are of utmost importance. These include the components of the normal unit vector of fitted planes; the segment size, reflectance values, inclination angles and orientation. Segment size helps identify rubble zones in conjunction with mean reflectance, inclination angles helps identify tilt in walls, orientation helps identify tilt in roofs and also pairs of gable roofs.
- How will features be combined to define damaged buildings?
  - Given that in mapping science roof features of identified buildings form the basis for spatial planar representation of buildings they were used to define building units. The polygon defined by the convex hull based on roof edge coordinates was projected onto the zero planes. Next, all walls, roofs and rubble within and around 1.25m of its edge were clustered and their properties analysed to give the overall damage status for the

building in question. This worked for roofed buildings, however in situations lacking roofs then rubble was used to define the second set of building units. This was informed by the reasoning that collapsed buildings have no roofs on top hence the convex hull of rubble units projected on 2D plane was used to cluster any walls within 2 times its standard distance, based on which the overall damage status was defined.

- How will the classification process be implemented?
  - This involved clustering identified roofs, walls or rubble as defined in section 5.4 and analysing the combination of properties in line with the practical definition of the damage classes in section 5.6.
- What factors will affect the classification process?
  - The classification process is affected first by availability of total coverage especially of available data given walls identified first then roofs thus missing data on walls means missing capturing the roofs and related features. Further, given the variation in acquisition dates of the datasets what is existent in one datasets in a particular form may be varied on the other dataset. Features for entity extraction (section 4.5) also affect the classification process as poorly defined features may lead to improper target object extraction consequently leading to inappropriate overall damage classification.
- How will accuracy of the classification process be implemented?
  - Accuracy is implemented based on identified versus non identified target objects. Sample target objects are compared with the classification target object results to see if all are found in the correct form and position. However, no ground truth data existed for the defined damage classes hence the process was analysed visually by overlaying the classification results onto the supplied geo-eye ortho image.

7.2. Conclusions

The conclusions for this research are as summarised below.

1. Damage assessment can be greatly improved by use of recognised damage classification catalogues. The advantage being that any party that requires the outcome of such a process will easily incorporate it because of the ease of understanding the damage categories used, in this case employed based on the damage catalogue.
2. Point cloud data coverage and noise levels influence the extraction of target building objects. In cases of no coverage or higher noise levels, the chances of erroneous extraction and classification of objects of interest automatically affects the final damage assessment results. A key pointer being in the complete coverage of target objects or buildings within the site of interest as a result of both roof and façade is captured in the combined use of ALS and AOP point cloud data.
3. Based on the results, the feasibility of automating earthquake building damage assessment procedures involving combined ALS and AOP data input has been proven. This is exemplified by basic implementation of the classification process in form of a coded algorithm with constraints based on unique separating features sourced from the results of defining features peculiarly captured by the respective input point cloud data. This shows the ability to provide quick assessment of earthquake affected sites and assist responsive disaster management teams can be easily effected.
4. Based on the approach of analysing the target objects directly in relation to the site of interest, the research shows that individual characteristics of target objects can be analysed based on which dataset provides satisfactory entity for its identification and classification. Evidence on this is by considering the two entities employed in this classification process where plane segments were

preferred for wall and roof features while connected component clusters were preferred for rubble and vegetation identification and extraction This is further exemplified by features identified and used in this study to classify target objects of interest. An example in case is the use of mean reflectance selectively from ALS point cloud to identify rubble zones and in a similar manner colour information provided key input in identifying urban tree crowns.

5. Rubble identification and extraction still places a considerable challenge to the classification process, as building construction materials vary thus more effort should be done to define rubble based on non concrete related structures.
6. Setting of threshold limits during segmentation and clustering process reveals the need to always analyse the nature of any site of interest, especially point cloud density before defining the distinct features.

7.3. Recommendations

Several recommendations were thought of as mentioned below.

1. There is need to always ensure complete coverage of availed data to ensure future classification processes cover the area of interest and identify target objects of interest their full entirety.

2. The threshold and constraints set in identifying roof and wall objects should be further analysed and more clues on how to improve their set up determined.

3. The use of the standard distance to link roof and wall segment features should be further researched on. This is so as it enables quick determination of relative positions of roof and wall objects without undergoing the rigorous topological relations exercise.

4. More research on damage assessment methods involving post earthquake data only should be encouraged to facilitate the quick requirement of damage response organisations that may be delayed by waiting for acquisition of pre-earthquake data. This is to avoid effects of confusion that bedevils all areas affected by earthquakes, especially in the period immediately after its occurrence.

5. Efforts should be made to encourage development of oblique positioned laser scanning and data acquisition devices that can fly closer to the surface, and have small sizes in form of unmanned aerial vehicles to help in automatic acquisition of facade view point cloud data.

LIST OF REFERENCES

Brunner, D., Lemoine, G., & Bruzzone, L. (2010). Earthquake Damage Assessment of Buildings Using VHR Optical and SAR Imagery. *Geoscience and Remote Sensing, IEEE Transactions on, 48*(5), 2403-2420. doi: 10.1109/tgrs.2009.2038274

DEC. (2012). HAITI EARTHQUAKE FACTS AND FIGURES Retrieved 04-01-2013, from http://www.dec.org.uk/haiti-earthquake-facts-and-figures

Dong, P., & Guo, H. (2011). A framework for automated assessment of post-earthquake building damage using geospatial data. *International Journal of Remote Sensing, 33*(1), 81-100. doi: 10.1080/01431161.2011.582188

Firchau, S., & Wiechert, A. (2005). Accurate On-Time Geo-Information for Disaster Management and Disaster Prevention by Precise Airborne Lidar Scanning. In P. Oosterom, S. Zlatanova & E. Fendel (Eds.), *Geo-information for Disaster Management* (pp. 109-119): Springer Berlin Heidelberg.

Furukawa, Y., & Ponce, J. (2010). Accurate, Dense, and Robust Multiview Stereopsis. *Pattern Analysis and Machine Intelligence, IEEE Transactions on, 32*(8), 1362-1376. doi: 10.1109/tpami.2009.161

Gerke, M. (2009). Dense matching in high resolution oblique airborne images. *In: CMRT09: Object extraction for 3D city models, road databases and traffic monitoring : concepts, algorithms and evaluation, Paris, 3-4 September 2009. / ed by U. Stilla, F. Rottensteiner and N. Paparoditis. ISPRS, 2009. pp 77-82.*

Gerke, M., & Kerle, N. (2011). Automatic Structural Seismic Damage Assessment with Airborne Oblique Pictometry (c) Imagery. [Article]. *Photogrammetric Engineering and Remote Sensing, 77*(9), 885-898.

Grünthal, G. (1998). De European Macroseismic Scale in verkorte vorm. In G. Grünthal (Ed.). Luxembourg: Centre Européen de Géodynamique et de Séismologie.

Grussenmeyer, P., & Al Khalil, O. (2002). Solutions for exterior orientation in photogrammetry: A review. [Review]. *Photogrammetric Record, 17*(100), 615-634. doi: 10.1111/0031-868x.00210

Guo, H., Lu, L., Ma, J., Pesaresi, M., & Yuan, F. (2009). An improved automatic detection method for earthquake-collapsed buildings from ADS40 image. *Chinese Science Bulletin, 54*(18), 3303-3307. doi: 10.1007/s11434-009-0461-3

Hobart, M. K. (2012). 2004 Indonesia Tsunami Maps Retrieved 04-01-2013, 2013, from http://geology.com/articles/tsunami-map.shtml

Karbø, N., & Schroth, R. (2009). Oblique Aerial Photography: A Status Review. In D. Fritsch (Ed.), Photogrammetric Week 2009 (pp. 119-125). Stuttgart: Institute for Photogrammetry. Retrieved from http://www.ifp.uni-stuttgart.de/publications/phowo09/140Karbo.pdf.

Krispijn, S. (2009). Accurate polygon extension. Retrieved from http://www.mathworks.nl/matlabcentral/fileexchange/21925-accurate-polygon-extension/content/extendPoly.m

Lodhi, M. A. (2013). Multisensor imagery analysis for mapping and assessment of 12 January 2010 earthquake-induced building damage in Port-au-Prince, Haiti. [Article]. *International Journal of Remote Sensing, 34*(2), 451-467. doi: 10.1080/01431161.2012.712226

McEntire, D., Souza, J., Collins, M., Peters, E., & Sadiq, A.-A. (2012). An introspective glance into damage assessment: challenges and lessons learned from the Paso Robles (San Simeon) earthquake. *Natural Hazards, 61*(3), 1389-1409. doi: 10.1007/s11069-011-0071-7

Morgan, M. F. (1999). *Building extraction from laser scanning data.* ITC, Enschede.

Nateghi-A, F. (1996). Assessment of wind speeds that damage buildings. *Natural Hazards, 14*(1), 73-84. doi: 10.1007/bf00229912

NCDC. (2012). Hurricane Katrina Retrieved 04-01-2013, from http://www.ncdc.noaa.gov/special-reports/katrina.html

Ogawa, N., & Yamazaki, F. (1999). *Image interpretation of building damage due to the 1995 Hyogoken-Nanbu Earthquake using Aerial photographs.* Paper presented at the Asia-Pacific Symposium on Structural Reliability and Its Applications, Taipei, Taiwan.

Oliveira, C. S., & Campos-Costa, A. (2006). Overview on Earthquake Hazard Assessment — Methods and New Trends. In C. Oliveira, A. Roca & X. Goula (Eds.), *Assessing and Managing Earthquake Risk* (Vol. 2, pp. 15-46): Springer Netherlands.

Oude Elberink, S. J., Shoko, M., Fathi, S. A. M., & Rutzinger, M. (2011). Detection of collapsed buildings by classifying segmented airborne laser scanner data. *In: ISPRS workshop laser scanning 2011, Calgary, Canada, 29-31 August 2011 / ed. by D.D. Lichti and A.F. Habib. - : International Society for Photogrammetry and Remote Sensing (ISPRS), 2011. - (International Archives of Photogrammetry and Remote Sensing : IAPRS : ISPRS ; XXXVIII-5/W12). 6 p.*

Pistrika, A., & Jonkman, S. (2010). Damage to residential buildings due to flooding of New Orleans after hurricane Katrina. *Natural Hazards, 54*(2), 413-434. doi: 10.1007/s11069-009-9476-y

Ponti, M. P. (2013). Segmentation of Low-Cost Remote Sensing Images Combining Vegetation Indices and Mean Shift. *Geoscience and Remote Sensing Letters, IEEE, 10*(1), 67-70. doi: 10.1109/lgrs.2012.2193113

Qi, H., & Altinakar, M. S. (2011). Simulation-based decision support system for flood damage assessment under uncertainty using remote sensing and census block information. *Natural Hazards, 59*(2), 1125-1143. doi: 10.1007/s11069-011-9822-8

Rezaeian, M., & Gruen, A. (2007). Automatic Classification of Collapsed Buildings Using Object and Image Space Features

Geomatics Solutions for Disaster Management. In J. Li, S. Zlatanova & A. G. Fabbri (Eds.), (pp. 135-148): Springer Berlin Heidelberg.

Rottensteiner, F., Trinder, J., Clode, S., & Kubik, K. (2007). Building detection by fusion of airborne laser scanner data and multi-spectral images: Performance evaluation and sensitivity analysis. *ISPRS Journal of Photogrammetry and Remote Sensing, 62*(2), 135-149. doi: http://dx.doi.org/10.1016/j.isprsjprs.2007.03.001

Rutzinger, M., Rottensteiner, F., & Pfeifer, N. (2009). A Comparison of Evaluation Techniques for Building Extraction From Airborne Laser Scanning. *Selected Topics in Applied Earth Observations and Remote Sensing, IEEE Journal of, 2*(1), 11-20. doi: 10.1109/jstars.2009.2012488

Samet, H. (1990). *Applications of spatial data structures: Computer graphics, image processing, and GIS*: Addison-Wesley Longman Publishing Co., Inc.

Schweier, C., & Markus, M. (2006). Classification of collapsed buildings for fast damage and loss assessment. *Bulletin of Earthquake Engineering, 4*(2), 177-192. doi: 10.1007/s10518-006-9005-2

Schweier, C., Markus, M., & Steinle, E. (2004). Simulation of earthquake caused building damages for the development of fast reconnaissance techniques. [Article]. *Natural Hazards and Earth System Sciences, 4*(2), 285-293.

SDSC, U. o. C. (2012). Open Topography Retrieved 14-12-2012, 2012, from http://www.opentopography.org/index.php/about/

Sirmacek, B., & Unsalan, C. (2008, 27-29 Oct. 2008). *Building detection from aerial images using invariant color features and shadow information.* Paper presented at the Computer and Information Sciences, 2008. ISCIS '08. 23rd International Symposium on.

Sithole, G. (2004). *Segmentation and classification of airborne laser scanning data : also as e-book.* 59, Nederlandse Commissie voor Geodesie (NCG), Delft. Retrieved from http://www.ncg.knaw.nl/Publicaties/Geodesy/pdf/59Sithole.pdf

Sithole, G., & Vosselman, G. (2004). Experimental comparison of filter algorithms for bare-Earth extraction from airborne laser scanning point clouds. *ISPRS Journal of Photogrammetry and Remote Sensing, 59*(1–2), 85-101. doi: 10.1016/j.isprsjprs.2004.05.004

Sithole, G., & Vosselman, G. (2005). Filtering of airborne laser scanner data based on segmented point clouds. *In: ISPRS 2005 : Vol. XXXVI Comm. 3 W19 proceedings of the ISPRS workshop laser scanning 2005, 12-15 September, Enschede ITC, The Netherlands / ed. by M.G. Vosselman and C. Brenner. Enschede; ITC, 2005. pp. 66-71.*

Sumer, E., & Turker, M. (2005, 9-11 June 2005). *Building damage detection from post-earthquake aerial imagery using building grey-value and gradient orientation analyses.* Paper presented at the Recent Advances in Space Technologies, 2005. RAST 2005. Proceedings of 2nd International Conference on.

Tian-Lin, W., & Ya-Qiu, J. (2012). Postearthquake Building Damage Assessment Using Multi-Mutual Information From Pre-Event Optical Image and Postevent SAR Image. *Geoscience and Remote Sensing Letters, IEEE, 9*(3), 452-456. doi: 10.1109/lgrs.2011.2170657

Tong, X., Hong, Z., Liu, S., Zhang, X., Xie, H., Li, Z., . . . Bao, F. (2012). Building-damage detection using pre- and post-seismic high-resolution satellite stereo imagery: A case study of the May 2008 Wenchuan earthquake. *ISPRS Journal of Photogrammetry and Remote Sensing, 68*(0), 13-27. doi: 10.1016/j.isprsjprs.2011.12.004

Van Aardt, J. A. N., McKeown, D., Faulring, J., Raqueno, N., Casterline, M., Renschler, C., . . . Gill, S. (2011). *Geospatial Disaster Response during the Haiti Earthquake: A Case Study Spanning Airborne Deployment, Data Collection, Transfer, Processing, and Dissemination* (Vol. 77). Bethesda, MD, ETATS-UNIS: American Society for Photogrammetry and Remote Sensing.

Vosselman, G. (2009). Advanced point cloud processing. *In: Photogrammetric Week '09 / ed. by. D. Fritsch. Heidelberg : Wichmann, 2009. ISBN 978-3-87907-483-9. pp. 137-146*.

Vosselman, G., & Maas, H.-G. (2010). *Airborne and terrestrial laser scanning*. GB: Whittles Publishing.

Vu, T. (2011). Building extraction from high-resolution satellite image for tsunami early damage estimation. *Applied Geomatics, 3*(2), 75-81. doi: 10.1007/s12518-010-0039-4

Xiao, J., Gerke, M., & Vosselman, G. (2012). Building extraction from oblique airborne imagery based on robust façade detection. *ISPRS Journal of Photogrammetry and Remote Sensing, 68*(0), 56-68. doi: http://dx.doi.org/10.1016/j.isprsjprs.2011.12.006

Xu, S., Oude Elberink, S., & Vosselman, G. (2012). Entities and features for classification of airborne laser scanning data in urban area. *ISPRS Ann. Photogramm. Remote Sens. Spatial Inf. Sci., I-4*, 257-262. doi: 10.5194/isprsannals-I-4-257-2012

Yusuf, Y., Matsuoka, M., & Yamazaki, F. (2001). Damage assessment after 2001 Gujarat earthquake using Landsat-7 satellite images. *Journal of the Indian Society of Remote Sensing, 29*(1), 17-22. doi: 10.1007/bf02989909